Genome Profiling for Aflatoxin B1 Resistance in *Saccharomyces cerevisiae* Reveals a Role for the CSM2/SHU Complex in Tolerance of Aflatoxin B_1-associated DNA Damage

Nick St. John[1.], Julian Freedland[1.], Henri Baldino[1.], Frank Doyle[1.], Cinzia Cera[1.], Thomas Begley[1.#], Michael Fasullo[1. *]

[1.]College of Nanoscale Science and Engineering

State University of New York Polytechnic Institute

257 Fuller Drive

Albany, New York 12203

[#]Present address: RNA Institute, State University of New York at Albany, 1400 Washington Ave, Albany, New York 12222

Public Depository of Data:

https://www.ncbi.nlm.nih.gov/geo/query/acc.cgi?acc=GSE129699.

Running Title: Yeast Resistance to AFB_1

Key words: genome profiling, aflatoxin, budding yeast, DNA damage tolerance

*Corresponding author:

Michael Fasullo

College of Nanoscale Science and Engineering

State University of New York Polytechnic Institute

257 Fuller Drive

Albany, New York 12203

Phone: (518) 956-7385

e-mail: mfasullo@sunypoly.edu

ABSTRACT Exposure to the mycotoxin aflatoxin B1 (AFB_1) strongly correlates with hepatocellular carcinoma. P450 enzymes convert AFB_1 into a highly reactive epoxide that forms unstable 8,9-dihydro-8-(*N*7-guanyl)-9-hydroxyaflatoxin B1 (AFB_1-N^7-Gua) DNA adducts, which convert to stable mutagenic AFB_1 formamidopyrimidine (FAPY) DNA adducts. In CYP1A2-expressing budding yeast, AFB_1 is a weak mutagen but a potent recombinagen. However, few genes have been identified that confer AFB_1 resistance. Here, we profiled the yeast genome for AFB_1 resistance. We introduced the human CYP1A2 into ~90% of the diploid deletion library, and pooled samples from CYP1A2-expressing libraries and the original library were exposed to 50 μM AFB_1 for 20 hs. By using next generation sequencing to count molecular barcodes, we identified 85 AFB_1 resistant genes from the CYP1A2-expressing libraries. While functionally diverse genes, including those that function in proteolysis, actin reorganization, and tRNA modification, were identified, those that function in post-replication DNA repair and encode proteins that bind to DNA damage were over-represented, compared to the yeast genome, at large. DNA metabolism genes included those functioning in DNA damage tolerance, checkpoint recovery and replication fork maintenance, emphasizing the potency of the mycotoxin to trigger replication stress. Among genes involved in error-free DNA damage tolerance, we observed that *CSM2*, a member of the *CSM2(SHU)* complex, functioned in AFB_1-associated sister chromatid recombination while suppressing AFB_1-associated mutations. These studies thus broaden the number of AFB_1 resistant genes and have elucidated a mechanism of error-free bypass of AFB_1-associated DNA adducts.

INTRODUCTION

The mycotoxin aflatoxin B1 (AFB_1) is a potent hepatocarcinogen. The signature p53 mutation, p53-Ser249, is often present in liver cancer cells from hepatocellular carcinoma (HCC) patients from AFB_1-exposed areas, suggesting that AFB_1 is a potent carcinogen because it is a genotoxin (Hsu et al., 1991; Shen and Ong, 1996). A mutagenic signature associated with AFB_1 exposure has been identified in HCC (Chawanthayatham et al., 2017; Huang et al., 2017). However, AFB_1 is not genotoxic *per se* but is metabolically activated by P450 enzymes, such as CYP1A2 and CYP3A4 (Crespi et al., 1991; Eaton and Gallagher, 1994; Gallagher et al., 1996), to form a highly reactive AFB_1-8-9-epoxide (Baertschi et al., 1988). The epoxide reacts with protein, RNA, and DNA, yielding the unstable 8,9-dihydro-8-(*N*7-guanyl)-9-hydroxyaflatoxin B1 (AFB1-N^7-Gua) adducts that convert into stable AFB_1-formamidopyrimidine (FAPY) adducts (Essigman et al., 1977; Lin et al., 1977; Croy et al., 1981). The anomers of the AFB_1-FAPY-DNA adduct block DNA replication or cause mutations in *Escherichia coli* (Smela et al., 2002; Brown et al., 2006) and *in vitro* (Lin et al, 2014). Metabolically active AFB_1 can also indirectly damage DNA through oxidative stress (Shen et al., 1995; Bedard and Masey, 2006; Bernabucci et al., 2011; Singh et al., 2015). Identifying genes that repair AFB_1-associated DNA damage could help identify which individuals are at elevated risk for HCC. However, epidemiological data has been inconsistent, and only a few candidate DNA repair genes have been proposed, such as XRCC1(Pan et al., 2011, Xu et al., 2015), XRCC3 (Long et al., 2008; De Mattia et al., 2017) and XRCC4 (Long et al., 2013).

AFB_1 resistance genes have been identified from model organisms, revealing mechanisms by which AFB_1-associated DNA adducts can be both tolerated and excised. Both prokaryotic and eukaryotic nucleotide excision repair (NER) pathways function to remove AFB_1-associated DNA adducts (Leadon, et al, 1981; Alekseyev et al., 2004; Bedard and Massey, 2006). Recently, the base excision repair gene (BER) NEIL1 has been implicated in direct repair AFB_1-associated DNA adducts (Vartanian et al., 2017). To tolerate persistent AFB_1-associated DNA lesions, translesion polymerases in yeast, such as those encoded by *REV1* and *REV7*, and in mouse, such as Polζ, confer resistance and may promote genome stability (Lin et al., 2014).

While yeast do not contain endogenous P450 genes that can metabolically activate AFB_1 into an active genotoxin (Sengstag et al., 1996; Van Leeuwen et al., 2013, Fasullo et al., 2014), human CYP1A2 can be expressed in yeast cells (Sengstag et al., 1996; Fasullo et al., 2014). Interestingly, metabolically activated AFB_1 is a potent recombinagen but weak mutagen (Sengstag et al., 1996). CYP1A2-activated AFB_1 reacts to form both the unstable AFB_1-N^7-Gua adducts and the stable AFB_1-FAPY DNA adducts (Fasullo et al., 2008). The AFB_1-associated DNA damage, in turn, triggers a robust DNA damage response that includes checkpoint activation (Fasullo et al., 2008), cell cycle delay (Fasullo et al., 2010), and the transcriptional induction of stress-induced genes (Keller-Seitz et al., 2004; Guo et al., 2006). Profiles of the transcriptional response to AFB_1 exposure reveals induction of genes in growth and checkpoint signaling pathways, DNA and RNA metabolism, and protein trafficking (Keller-Seitz et al, 2004; Guo et al., 2006). While genes involved in recombinational repair and DNA damage tolerance confer AFB_1 resistance (Keller-Seitz et al., 2004; Fasullo et al, 2010;

Guo et al, 2005), it is unclear the functional significance of many genes in the stress induced pathways in conferring resistance since transcriptional induction is not synonymous with conferring resistance (Birrell et al., 2004).

In this study, we profiled the yeast genome for AFB_1 resistance. We asked which genes confer AFB_1 resistance in the presence or absence of human CYP1A2 expression by screening the non-essential diploid collection by high throughput sequencing of molecular barcodes (Pierce et al., 2006; St Onge et al. 2007; Smith et al., 2010). While we expected to identify NER, recombinational repair, and DNA damage tolerance genes, which had previously been identified (Keller-Seitz et al., 2004; Fasullo et al, 2010; Guo et al, 2005), our high throughput screen identified novel genes involved in AFB_1 resistance. These included genes involved in Rad51 assembly, cell cycle progression, RNA metabolism, and oxidative stress. Our results thus underscore the importance of recombination in both mutation avoidance and in conferring AFB_1 resistance.

Materials and Methods

Strains and plasmids

Yeast strains were derived from BY4741, BY4743 (Brachman et al., 1998) or YB204 (Dong and Fasullo, 2003); all of which are of the S288C background (supplemental Table 1). The BY4743 genotype is *MAT*a/α *his3*Δ*1/his3*Δ*1 leu2*Δ*0/leu2*Δ*0 LYS2/lys2*Δ*0 met15*Δ*0/MET15 ura3*Δ*0/ura3*Δ*0.* The diploid and haploid homozygous deletion libraries were purchased from Open Biosystems, and are now available from

Dharmacon (http://dharmacon.gelifesciences.com/cdnas-and-orfs/non-mammalian-cdnas-and-orfs/yeast/yeast-knockout-collection/). The pooled diploid homozygous deletion library (n = 4607) was a gift of Chris Vulpe (University of Florida).

To construct the *csm2 rad4* and *csm2 rad51* double mutants, we first obtained from haploid *csm2* strain (YA288, supplemental Table 1) from the haploid BY4741-derived deletion library. We introduced the *his3* recombination substrates (Fasullo and Davis, 1987) to measure unequal sister chromatid exchange (SCE) in the *csm2* mutant by isolating the meiotic segregant YB558 from a diploid cross of YB204 with YA288. This *csm2* strain (YB558) was subsequently crossed with *MAT*α *rad4::NatMX* (YA289) and the *csm2::KanMX rad4::NatMX* meiotic segregant (YB600) was obtained. The *rad51 csm2* double mutant was made by one step gene disruption (Rothstein, 1983) using the *Bam*H1 fragment *rad51*Δ (Shinohara et al., 1992) to select for Ura^+ transformants in YB558.

Using LiAc-mediated gene transformation we introduced human CYP1A2 into BY4741, *csm2*, *rad4*, *rad51*, *csm2 rad51*, and *csm2 rad4* strains. The CYP1A2-expression plasmid, pCS316, was obtained by CsCl centrifugation (Ausubel, 1994) and the restriction map was verified based on the nucleotide sequence of the entire plasmid. An alternative CYP1A2-expression plasmid, pCYP1A2-NAT2 was constructed by removing the hOR sequence from pCS316 and replacing it with a *Not*1 fragment containing the human NAT2.

Media and chemicals

Standard media were used for the culture of yeast and bacterial strains (Burke et al., 2000). LB-AMP (Luria broth containing 100 µg/ml ampicillin) was used for the culture of the bacterial strain DH1 strain containing the vector pCS316. Media used for the culture of yeast cells included YPD (yeast extract, peptone, dextrose), SC (synthetic complete, dextrose), SC-HIS (SC lacking histidine), SC-URA (SC lacking uracil), and SC-ARG (SC-lacking arginine). Media to select for canavanine resistance contained SC-ARG (synthetic complete lacking arginine) and 60 µg/mL canavanine (CAN) sulfate, and media to select for 5-fluoroorotic acid (FOA) resistance contained SC-URA supplemented with 4x uracil and FOA (750 µg/ml), as described by Burke et al. (2000). FOA plates contained 2.2% agar; all other plates contained 2% agar. AFB_1 was purchased from Sigma Co., and a 10 mM solution was made in dimethyl sulfoxide (DMSO).

Measuring DNA Damage-Associated Recombination and Mutation Events

To measure AFB_1-associated genotoxic events, log phase yeast cells (A_{600}=0.5-1) were exposed to indicated doses of AFB_1, previously dissolved in DMSO. Cells were maintained in synthetic medium (SC-URA) during the carcinogen exposure. After the exposure, cells were washed twice in H_2O, and then plated on SC-HIS or SC-ARG CAN to measure unequal SCE or mutation frequency, respectively. An appropriate dilution was inoculated on YPD to measure viability (Fasullo et al., 2008).

Construction of CYP1A2-expressiong library

To introduce CYP1A2 (pCS316, Sengstag et al., 1996, and pCYP1A2_NAT2) into the yeast diploid deletion collection, we used a modified protocol for high throughput yeast transformation in 96-well plates (Gietz and Schiestl 2006). In brief, FOA^R isolates were isolated from each individual strain in the diploid collection and inoculated in 96-well plates, each containing 100 μl of YPD medium. After incubation over-night at 30°C, plates were centrifuged, washed in sterile H_2O, and resuspended in one-step buffer (0.2 N LiAc, 100 mM DTT, 50% PEG, MW 3300, 500 μg/ml denatured salmon sperm DNA). After addition of 1 μg pCS316 and incubation for 30 minutes at 30°C, 10 μl were directly inoculated on duplicate SC-URA plates. Two Ura^+ transformants were chosen corresponding to each well and frozen in SC-URA 0.75% DMSO. We introduced the CYP1A2-containing plasmids into approximately 90% of the deletion collection.

Functional profiling of the yeast genome

The CYP1A2-expressing libraries were pooled and frozen in SC-URA medium containing 0.75% DMSO (n = 4150). The pooled cells (100 μl) were added to 2 ml of SC-URA and allowed to recover for two hours. Cell were then diluted to A_{600} = 0.85 in 2 ml of SC-URA and exposed to either 50 μM AFB_1 in 0.5% DMSO, and 0.5% DMSO alone. Cells were then incubated with agitation at 30°C for 20 hs. Similarly, the pooled BY4743 library (n = 4607) was directly diluted to A_{600} = 0.85 in YPD and also exposed to 50 μM AFB_1 and DMSO for 20 hs. Independent triplicate experiments were performed for each library and each chemical treatment.

After AFB_1 exposure, cells were washed twice in sterile H_2O and frozen at -80^oC. Cells were resuspended in 10 mM Tris-HCl, 1 mM EDTA, 100 mM NaCl, 2% Triton X-100, 1% SDS, pH 8 and DNA was isolated by "smash and grab (Hoffman and Winston. 1987)." Barcode sequences, which are unique for each strain in the deletion collection (Giaever et al., 2002; Giaever et al, 2004), were amplified by PCR using a protocol described by Smith et al. (2010). The primers used for amplification are listed in the Supplemental Table 2. 125 bp PCR products were then isolated from 10% polyacrylamide gels by diffusion in 0.5M NH_4Ac 1 mM EDTA for 24 hs (30^oC) followed by ethanol precipitation. The DNA was quantified after being resuspended in Tris EDTA pH 7.5 and the integrity of the DNA was verified by electrophoresis on 10% polyacrylamide. Equal amounts of DNA were pooled from treated and untreated samples. The uptags were then sequenced using the Illumina Platform at the University Buffalo Genomics and Bioinformatics Core (Buffalo, New York). Sequence information was then uploaded to an accessible computer server for further analysis. The software to demultiplex the sequence information, match the uptag sequences with the publish ORFs, and calculate the statistical significance of the differences in log2N ratios was provided by F. Doyle. Tag counts were analyzed with the TCC Bioconductor package (Sun et al., 2013) using TMM normalization (Robinson and Oshlock, 2010) and the edgeR test method (Robinson et al., 2009)**.** Statistical significance was determined using Linux software. Data files have been deposited in the Gene Expression Omnibus database, GSE129699.

Over-enrichment analysis.

Gene Ontology (GO) categories were identified by a hypergeometric distribution with freely available software from University of Toronto (http://funspec.med.utoronto.ca/), YeastMine database (http://yeastmine.yeastgenome.org/), and Panther (http://pantherdb.org/tools/) with a P value cutoff of < 0.05 (Cherry et al., 2012, Mi et al., 2016). The AFB_1 sensitivity of selected of mutants corresponding to gene ontology groups were verified by growth curves.

Western blot analysis

Expression of CYP1A2 was determined by Western blots and MROD assays. Cells were inoculated in SC-URA medium. Cells in log growth phase (A_{600} = 0.5–1) were concentrated and protein extracts were prepared as previously described by Foiani et al. (1994). Proteins were separated on 10% acrylamide/0.266% bis-acrylamide gels and transferred to nitrocellulose membranes. Human CYP1A2 was detected by Western blots using goat anti-CYP1A2 (Abcam), and a secondary bovine anti-goat antibody. For a loading control on Western blots, β-actin was detected using a mouse anti-β-actin antibody (Abcam 8224) and a secondary goat anti-mouse antibody. Signal was detected by chemiluminescence, as in previous publications (Fasullo et al., 2014).

Measuring CYP1A2 enzymatic activity

We measured CYP1A2 enzymatic activity using a modified protocol described by Pompon *et al.* (1996). In brief, cells obtained from 100 ml of selective media were pelleted and resuspended in 5 ml Tris EDTA KCl (pH 7.5, TEK) buffer. After five minute

incubation at room temperature, cells were pelleted, resuspended in 1 ml 0.6 M Sorbitol Tris pH 7.5, and glass beads were added. Cells were lysed by agitation. The debris was pelleted at 10,000 x g at 4^{o}C, and the supernatant was diluted in 0.6 M Sorbitol Tris pH 7.5 and made 0.15 M in NaCl and 1% in polyethylene glycol (MW 3350) in a total volume of 5 ml. After incubation on ice for 1 hr. and centrifugation at 10,000 rpm for 20 minutes, the precipitate was resuspended in Tris 10% glycerol pH 7.5, and stored at -80^{o}C.

CYP1A2 enzymatic activity was measured in cell lysates by quantifying 7-methoxyresorufin O-demethylase (MROD) activities (Fasullo et al., 2014), using a protocol similar to that quantifying ethoxyresorufin O-deethylase (EROD) activity (Eugster et al., 1992; Sengstag et al., 1994). The buffer contained 10 mM Tris pH 7.4, 5μM methoxyresorufin (Sigma) and 500 μM NADPH. The production of resorufin was measured in real-time by fluorescence in a Tecan plate reader, calibrated at 535 nm for excitation and 580 nm for absorption, and standardized using serial dilutions of resorufin. The reaction was started by the addition of NADPH and resorufin was measured at one minute intervals during the one hour incubation at 37^{o}C; rat liver microsomes (S9) were used as a positive control while the reaction without NADPH served as the negative control. Enzyme activities were measured in duplicate for at least two independent lysates from each strain and expressed in pmol/min/mg protein.

Growth assays in 96 well plate to measure AFB_1 sensitivity

In brief, individual saturated cultures were prepared for each yeast strain. Cell density was adjusted to ~0.8 x 10^7 cells/ml for all cultures. We maintained the cells in selective medium (SC-URA). In each microtiter well, 95 μl of media and 5 μl of cells (8 x 10^4 cells) were aliquoted in duplicate for blank, control and experimental samples. For experimental samples, we added AFB_1, dissolved in DMSO, for a final concentration of 50 μM and 100 μM. The microtiter dish was placed in a plate reader that is capable of both agitating and incubating the plate at 30° C, as previously described (Fasullo et al., 2010; Fasullo et al., 2014). We measured the A_{600} at 10 minute intervals, for a total period for 24 hs, 145 readings. Data at 1hr intervals was then plotted. To avoid evaporation during the incubation, the microtiter dishes were sealed with clear optical tape (Fasullo et al, 2010). To calculate area under the curve (AUC), we used a free graphing application (https://www.padowan.dk/download/), and measured the time interval between 0-20 hs, as performed in previous publications (O'Connor et al., 2012). Statistical significance was determined by the Student's *t*-test, assuming constant variance between samples.

To determine epistasis of AFB_1-resistant genes, we calculated the deviation ε according to $\varepsilon = W_{xy} - W_x \times W_y$, where W_x and W_y are the fitness coefficients determined for each single mutant exposed to AFB_1 and W_{xy} is the product. Fitness was calculated by determining the generation time of both the single and double mutants over three doubling times. Zero and negative values are indicative of genes that do not interact or participate in the same pathway to confer fitness (St. Onge et al., 2007).

Data Availability

All yeast strains and plasmids are available upon request and are detailed in STable 1. Three supplementary tables and two supplementary figures have been deposited in figshare. Next generation sequencing data (NGS) of barcodes are available at GEO with accession number GSE129699.

Results:

We used three BY4743-derived libraries to profile the yeast genome for AFB_1 resistance. The first was a pooled library of 4607 yeast strains, each strain containing a single deletion in a non-essential gene (Jo et al, 2009). The second was a pooled library of approximately 4900 strains each containing individual deletions in non-essential genes and was made by introducing pCS316 into each strain by yeast transformation (Figure 1). The third was a pooled library of approximately 5000 strains expressing both CYP1A2 and NAT2. By calculating area under the growth curves, we determined that the D_{10} for wild type BY4743 expressing CYP1A2 was 50 μM AFB_1 while the D_{16} for BY4743 expressing CYP1A2 was 100 μM (Figure 1). The D_{10} for wild type BY4743 expressing CYP1A2 with the hOR was the same as in BY4743 cells expressing CYP1A2 and NAT2. To confirm metabolic activation of AFB_1 into a potent genotoxin, we showed that growth of the *rad52* diploid mutant was significantly impaired (Figure 1). The non-linear relationship between dose and lethality is consistent with previous results that the number of DNA adducts do not linearly increase with increasing AFB_1 concentrations (Fasullo et al., 2008). Cells that did not express CYP1A2 showed slight growth delay after cells were exposed to 100 μM AFB_1 (Figure 1).

Confirmation of CYP1A2 activity

To confirm that CYP1A2 was both present and functional in the library, we performed Western blots and MROD assays, as in previous studies (Fasullo et al., 2014; Figure 1). Two independent assays were performed for five different ORFs (*RAD2, RAD18, RAD55, OGG1, MRC1*); the average MROD result was 5-10 units

pmol/sec/mg protein. These results are similar to what was observed for the wild type BY4743 (Fasullo et al., 2014) and for various haploid mutants (Guo et al., 2005). These studies indicate that CYP1A2 is active in diploid strains and can be detected by Western blots in BY4743-derived strains containing pCS316, in agreement with previous studies (Guo et al., 2005).

Identification of Genes by Barcode Analysis

We initially grouped AFB_1 resistance genes into: 1) those that confer resistance to AFB_1 without CYP activation, and 2) those that confer resistance to P450-activated AFB_1. After exposing cells to 50 μM AFB_1, we identified barcodes for approximately 51% and 89% of the genes from pooled deletion library with and without CYP1A2, respectively (for complete listing, see https://www.ncbi.nlm.nih.gov/geo/query/acc.cgi?acc=GSE129699).One gene, *CTR1*, was identified from the pooled library that did not express CYP1A2; this gene functions in high-affinity copper and iron transport (Dancis et al., 1994), and its human homolog confers drug resistance (Furukawa et al., 2008), indicating that *CTR1* is involved in xenobiotic transport. We speculate that higher AFB_1 concentrations are required to identify additional resistance genes in the yeast library lacking metabolic activation.

Using the same stringent assessment ($q < 0.1$), in three independent screens, we identified 95 genes that confer AFB_1 resistance in cells expressing CYP1A2, of which 85 genes have been ascribed a function. Of these, 15 DNA repair genes (18%) were identified (Table1) and another 70 genes have diverse functions (Table 2). The gene that scored the most highly significant was *RAD54*. Five highly significant genes,

participating in nucleotide excision repair, DNA damage tolerance, and ribosome assembly were twice found. An additional five genes were found that that were highly significant ($q < 0.1$) in one screen and significant in another screen ($p < 0.05$). Among these were those involved in proteolysis (*CUE1*), vacuolar acidification (*VOA1*), cell cycle progression (*FKH2*), DNA recombinational repair (*RAD55*) and DNA damage tolerance *(RAD18*). Selected genes were confirmed by growth curves (Figure 2); AUCs for additional genes are listed in supplemental Figure 1.

According Yeast GO-Slim Process and Funspec MIPS GO grouping, resistance genes included those that function in the DNA damage response, DNA repair, recombination, and DNA damage stimulus, tRNA modifications, carbohydrate metabolism, and cell cycle progression; the top fifteen GO groups are shown in Table 3 (for full list, see supplemental Table 3). Carbohydrate metabolism genes that function in cell wall maintenance and glycogen metabolism were previously identified to confer resistance to a variety of toxins, such as benzopyrene and mycophenolic acid (O'Connor et al., 2012). Other genes involved in carbohydrate metabolism, such as *GRE3* that encodes aldose reductase, could have a direct role in detoxification and is induced by cell stress (Barski et al., 2008). Genes involved in rearrangement of the cellular architecture include *BIT2*, *AKL1* and *PPG1*; these genes function to rearrange the cellular architecture when cells are stressed (Schmidt et al., 1996). Thus, among AFB_1 resistant genes are those that function to maintain structural integrity by affecting the cytoskeletal and cell wall architecture.

Other gene ontology groups encompass mitochondrial maintenance and response to oxidative stress, and RNA metabolism and translation (supplemental Table 3). Genes

involved in mitochondrial function and response to oxidative stress include *TRX3*, *MRPL35*, *MIX23*, *MIS1*; *TRX3* (thioredoxin reductase) functions to reduce oxidative stress in the mitochondria (Greetham and Grant, 2009). RNA metabolism genes include those that function tRNA modifications, including *MIS1, TRM9, DUS1,* and *RIT1* and RNA translation, such as *TMA20*. *TRM9* confers resistance to alkylated DNA damage, and links translation with the DNA damage response (Begley et al., 2007). These genes are consistent with the notion that AFB_1 causes oxidative damage and that mitochondria are targets of AFB_1-induced DNA damage.

In grouping genes according to cellular components (Yeast Mine), DNA repair complex was readily identified. Among the DNA repair complex was the Shu complex, and the NER complex I and II complex (Table 4). However, other interesting complexes that were identified included the glycosidase II complex, and the CK2 complex. Because DNA repair and DNA damage response genes were most prominent of the GO groups, we focused on the function of these genes in conferring AFB_1 resistance. As expected, these genes included those in DNA recombination (*RAD54, RAD55*), nucleotide excision repair (*RAD1, RAD4, RAD10*), and DNA damage tolerance (*RAD5, RAD18, REV1, REV3*). Many of these genes function in DNA damage tolerance both by directly interacting in the pathway and by affecting cell cycle progression. For example, *PSY2* and *CKB2* (Toczyski et al., 1997) promote cell cycle progression after cell cycle delay or arrest caused by stalled forks or double-strand breaks, respectively.

To determine which GO biological processes and protein functions were most enriched among the AFB_1 resistant genes we used the Panther software (Mi et al., 2016). Approximately 75% of the AFB_1 resistant genes were involved in response to

stress (Figure 3). A significant fraction of these genes also participate in DNA damage tolerance, including DNA post-replication repair and error-free and error-prone replication (Table 5). In classifying protein functions, we analyzed whether hydrolases, nucleases, phosphatases, DNA damage binding were more enriched among the 85 AFB_1 resistant genes, compared to the genome, at large (Figure 3). Of these groups, only DNA damage binding demonstrated a significant difference ($P < 0.05$).

To further determine the strength of the interactions among the AFB_1 resistance genes, we performed interactome mapping, using STRING software (https://string-db.org/, Szklarczyk et al., 2019), which associates proteins according to binding, catalysis, literature-based, and unspecified interactions (Figure 4). The interactome complex in yeast included 86 nodes and 162 edges with a 3.77 average node degree. Besides the NER complexes, Individual complexes included the Shu complex, the Glucosidase II complex, and the protein kinase CK2 complex (Table 4); the glucosidase II complex is conserved in mammalian cells (Figure 4), While the strength and number of these interactions was particularly strong among the DNA repair genes, other interactions were elucidated, such as the interactions of protease proteins with cell cycle transcription factors and cyclins (Figure 4).

Since many known AFB_1 resistance genes, which function in DNA repair and DNA damage tolerance pathways, were not present among highly significant genes ($q < 0.1$), we also used a less stringent ($p < 0.05$) qualifier to identify potential AFB_1 resistance genes. Among genes identified were additional members of the SHU complex, including *SHU1* and *SHU2*. These genes were confirmed by additional growth curves (supplemental Figure 2).

The SHU complex was previously identified as participating in error-free DNA damage tolerance and mutation avoidance (Shor et al., 2005; Xu et al, 2013). The complex confers resistance to alkylating agents, such as methyl methanesulfonate (MMS), and cross-linking agents, such as cisplatin, but not to UV and X-ray (Godin et al, 2015). We previously showed that while X-ray associated unequal SCE (SCE) was *RAD5*-independent (Fasullo and Sun, 2017), MMS and 4NQO-associated unequal SCE occurs by well-conserved *RAD5*-dependent mechanisms (Fasullo and Sun, 2017; Unk et al., 2010). We therefore postulated that the SHU complex suppresses AFB_1-associated mutagenesis while promoting AFB_1-associated template switching. We introduced pCS316 (CYP1A2) into both the haploid wild-type strain (YB204) and a *csm2* mutant (YB558, see supplemental Table 1) to measure frequencies of AFB_1-associated unequal SCE and *can1* mutations. Our results showed that while we observed a three-fold increase in SCE after exposure to AFB_1 in wild type strains, we observed less than a two-fold increase in sister chromatid exchange in the *csm2* mutant (Figure 5). However, we observed a net increase in AFB_1-associated Can^R mutations in the in *csm2* mutant, compared to wild type ($P < 0.05$). Average survival was only slightly higher in the wild type (51%) than in the *csm2* mutant (49%), but not statistically different ($P = 0.8$, N =4). We suggest that similar to MMS-associated DNA lesions, *CSM2* functions to suppress AFB_1-associated mutagenesis while promoting template switching of AFB_1-associated DNA adducts.

If *CSM2* participates in a *RAD51*-dependent recombinational repair pathway to tolerate AFB1-associated DNA lesions, then we would expect that *RAD51* would be epistatic to *CSM2* for AFB1 resistance (Glassner and Mortimer, 1984). We measured

AFB_1 sensitivity in the *csm2*, *rad51* and *csm2 rad51* haploid mutants compared to wild type, using growth curves (Figure 6). Our data indicate the *csm2 rad51* double mutant is no more AFB_1 sensitive compared to either *rad51* single mutants indicating that *CSM2* and *RAD51* are in the same epistasis group for AFB_1 sensitivity. In contrast, *csm2 rad4* double mutants are more sensitive to AFB_1 than either the *csm2* and *rad4* single mutants; the fitness measurement of the double mutant (0.071) is also less than the product of the *csm2* (0.34) and *rad4* (0.28) single mutants . These data indicate that *CSM2* participates in a *RAD51*-mediated pathway for AFB_1 resistance, and similar to *RAD51*, confers AFB_1 resistance in a *rad4* mutant (Fasullo et al., 2010).

Human orthologs for many essential yeast genes can directly complement the corresponding yeast genes (Kachroo et al., 2015). Human homologs are listed for 52 yeast AFB_1-resistant genes. (Table 6). These homologs include those for DNA repair, DNA damage tolerance, cell cycle, and cell maintenance genes. Several of these genes, such as the human *CTR1* (Zhou and Gitschier, 1997), can directly complement the yeast gene. Other DNA human DNA repair genes, such as those that encode *RAD54* (Kanaar et al., 1996), *RAD5* (Unk et al, 2010), and *RAD10* orthologs, can partially complement sensitivity to DNA damaging agents (Aggarwal and Brosh, 2012).

Discussion:

Human CYP1A2-mediated activation of the mycotoxin AFB_1 generates a highly reactive epoxide that interacts with DNA, RNA, and protein, forming adducts which interfere in replication, transcription, and protein function. Previous experiments have documented the role of checkpoint genes, RAD genes, and BER genes in conferring AFB_1 resistance in budding yeast (Keller-Seitz et al., 2004; Guo et al., 2005; Fasullo et al, 2010). The goal of this project was to identify additional AFB_1 resistance genes that may elucidate why AFB_1 is a potent yeast recombinagen but a weak mutagen (Sengstag et al., 1996).

Here, we profiled the yeast genome for AFB_1 resistance using three yeast non-essential diploid deletion libraries; one was the original library and the other two expressed human CYP1A2. We identified 96 resistance genes, of which 85 have been ascribed a function. These resistance genes reflect the broad range of functions, including cellular and metabolic processes, actin reorganization, mitochondrial responses, and DNA repair. Many of the DNA repair genes and checkpoint genes have been previously identified in screens for resistance to other toxins (Lee et al., 2005; Dela Rosa et al., 2017; Giaever and Nislow 2014). While, mitochondrial maintenance genes, and oxidative stress genes (Amici et al., 2007; Mary et al., 2012) are expected AFB_1 resistant genes based on studies of individual mutants (Fasullo et al, 2010; Guo et al., 2005), we also identified novel resistance genes that participate in DNA damage tolerance, both by modulating checkpoint responses and by recombination-mediated mechanisms. Of key importance, the CSM2/SHU complex (Shor et al., 2005) was required for AFB_1-associated sister chromatid recombination, underscoring the role of

recombination-mediated template switch mechanisms for tolerating AFB_1-associated DNA damage. Since many yeast genes are conserved in mammalian organisms (Bernstein et al, 2005), we suggest similar mechanisms for tolerating AFB_1-associated DNA damage may be present in mammalian cells.

We used a novel reagent consisting of a pooled yeast library expressing human CYP1A2, on a multi-copied expression vector. Because CYP1A2 activates AFB_1 when toxin concentration is low (Eaton and Gallagher, 1994), our modified yeast library mimicked AFB_1 activation when the toxin is present in low concentrations in the liver. One limitation of the screen in the CYP1A2-expressing library is that AFB_1-associated toxicity is not directly proportional to AFB_1 concentration (Fasullo et al., 2010); we speculate that CYP1A2 activity is the limiting factor. Although individual yeast strains expressed similar amounts of CYP1A2 activity from among the subset of deletion strains tested, it is still possible that profiling resistance among individual deletion strains is influenced by the stability or variable expression of the membrane-associated human CYP1A2 (Murray and Sa-Correia, 2001). Secondly, many DNA repair and checkpoint genes that were previously documented to confer resistance, such as *RAD52*, were not identified in the screen (Fasullo et al, 2010, Guo et al, 2006). One possible reason is that some, such as *rad52,* grow poorly (Figure 1, Fasullo et al, 2008), and we suspect that other slow-growing strains dropped out early in the time course of exposure. Future experiments will more carefully assess generation times needed to detect known resistance genes in the library expressing CYP1A2.

Because metabolically activated AFB_1 causes protein, RNA, and lipid damage (Weng et al., 2017), besides DNA damage, we expected to find a functionally diverse

set of AFB_1 resistance genes. Among AFB_1 resistant genes were those involved in protein degradation and ammonia transport, actin reorganization, tRNA modifications, ribosome biogenesis and RNA translation. Some genes encoding these functions, such as *BIT2* and *TRM9,* have important roles in maintaining genetic stability and in double-strand break repair (Begley, et al., 2007; Schmidt et al., 1996; Schonbrun et al, 2012; Shimada et al., 2013).Several genes, such as *PPG1*, are involved in glycogen accumulation; these genes are also required to enter the quiescent state (Li et al., 2015). Other genes are involved in cell wall synthesis, including *MNN10*, *SCW10* and *ROT2*; we speculate that cell wall synthesis genes confer resistance by impeding AFB_1 entrance into the cell, while genes involved in protein degradation in the ER may stabilize CYP1A2 and thus enhance AFB_1-conferred genotoxicity (Murray and Sa-Correia, 2001). Glucan and other cell wall constituents have also been speculated to directly inactivate AFB1, and yeast fermentative products are supplemented in cattle feed to prophylactically reduce AFB1 toxicity (Pereyra et al., 2013).

Although AFB_1-associated cellular damage is associated with oxidative stress (Amici et al., 2008; Liu and Wang, 2016; Mary et al., 2012) only a few yeast genes that confer resistance to reactive oxygen species (ROS) were identified in our screens. These genes included *TRX3*, *YND1*, *VPS13*, *BIT2, GTP1, FKH2, SHH3, NRP1,* and *BUD20*, which have a wide variety of functions (Bassler et al., 2012; Greetham and Grant, 2009; Schmidt et al., 1996). While known genes associated with oxidative stress and oxidative-associated DNA damage, such as *YAP1, SOD1*, and *APN1*, were not identified, other mitochondrial genes, such as *TRX3*, were identified. Guo et al. (2005) also showed that the haploid *apn1* mutant was not AFB_1 sensitive. We offer two

different explanations: first, the AFB_1-associated oxidative damage is largely localized to the mitochondria, and second, there may be redundant pathways for conferring resistance to AFB_1-associated oxidative damage, and therefore single genes were not identified. It is most likely the later as screens with oxidants (like t-BuOOH) also fail to identify expected antioxidant enzymes (Said et., al 2004).

A majority of the AFB_1 resistant genes belong to GO groups that include response to chemical, response to replication stress, and post replication repair. Proteins encoding functionally diverse genes, such as *RAD54*, *RAD5, GFD1*, *TMA20*, *SKG3*, *GRE3*, and *ATG29* (Table 3), are repositioned in the yeast cells during DNA replication stress (Tkach et al., 2012). The requirement for unscheduled DNA synthesis was illustrated by identifying genes involved in the DNA damage-induced expression of ribonucleotide reductase; these included *RNR3* and *TRM9*. *TRM9*, involved in tRNA modification, functions to selectively translate DNA damage-inducible genes, such as *RNR1* (Begley et al, 2007).

One unifying theme was that cell cycle progression and recovery from checkpoint-mediated arrest is a prominent role in mediating toxin resistance. *FKH2* functions as a transcription factor that promotes cell cycle progression and G_2-M progression. Other genes are involved in the modulation of the checkpoint response, such as *PSY2*. While *CKB1* and *CKB2* have broad functions, including histone phosphorylation and chromatin remodeling (Barz et al., 2003; Cheung et al., 2005), *CKB2* is also required for toleration of double-strand breaks (Toczyski et al., 1997; Guillemain et al., 2007), and thus may function for the toleration of AFB_1-associated

damage. These genes support the notion that some of the AFB_1-associated DNA adducts are well tolerated and can be actively replicated.

While we expected to identify individual genes involved in postreplication repair, such as *RAD5, REV1, REV3,* the *CSM2/PSY3* complex is novel. Absence of *CSM2* confers deficient AFB_1-associated SCE but higher frequencies of AFB_1-associated mutations, suggesting that *CSM2* functions to suppress AFB_1-associated mutations by *RAD51*-mediated template switch mechanisms (Fasullo et al., 2008; Guo et al., 2006). Consistent with this idea, *RAD51* is epistatic to *CSM2* in conferring AFB_1 sensitivity, while *rad4 cms2* double mutant exhibits synergistic AFB_1 sensitivity with respect to the single *rad4* and *csm2* single mutants. However, *rad4 rad51* mutants still exhibit more AFB_1 sensitivity than *rad4 csm2*, suggesting that *RAD51* may be involved in conferring resistance to other AFB_1-associated DNA lesions, such as double-strand breaks. We also expect that the *RAD51* paralogs, *RAD55* and *RAD57*, share similar AFB_1-associated functions with *RAD51*. Considering that *RAD57* is the XRCC3 ortholog, determining whether yeast *RAD51* paralogs suppress AFB_1-associated mutation will aid in identifying similar complexes in mammalian cells. Such complexes may elucidate why XRCC3 polymorphisms are risk factors in AFB_1-associated liver cancer (Long et al., 2008; Ji et al., 2015)

Human homologs of several of the identified yeast genes (Table 6) are, hyper-methylated, mutated, or over-expressed in liver disease and cancer. For example, mutations and promoter methylations of the human *RAD5* ortholog, Helicase-Like Transcription Factor (HLTF), are observed in hepatocellular carcinoma (Zhang, 2013; Dhont, 2016). Mutations in PRKCSH and GANAB, human orthologs of *GTB1* and

ROT2, are linked to polycystic liver disease (Porath et al., 2016; Perugorria and Banales, 2017). The *CKB2* ortholog, CSNK2B (Chua et al., 2017; Dotan et al., 2001; Zhang et al., 2015), is over-expressed in several liver cancers and therapeutics are currently in clinical trial (Gray et al., 2014, Li et al., 2017, Trembley et al., 2017). It is tempting to speculate that over-expression of CSNK2B also confers AFB_1 resistance.

Human homologs of other yeast genes have been correlated to the progression of other cancers, including colon cancer. These include the human homolog for *TRM9*, ALKB8, and the human homolog for *TMA20*, MCT1, which can complement translation defects of *tma20* mutants and has been implicated in modulating stress (Herbert and Shi, 2001) and double-strand break repair (Hsu et al., 2007). MCT-1 overexpression and p53 is noted to lead to synergistic increases in chromosomal instability (Kasiappan et al., 2009).

In summary, we profiled the yeast genome for AFB_1 resistance and identified novel genes that confer resistance. The novel genes included those involved in tRNA modifications, RNA translation, DNA repair, protein degradation, and actin reorganization. Genes that function in DNA damage response, post-replication repair, and DNA damage tolerance were over-represented, compared to the yeast genome. We suggest that the *CSM2* (SHU complex) functions to promote error-free replication of AFB_1-asociated DNA damage, and it will be interesting to determine whether mammalian orthologs of the SHU complex function similarly.

Acknowledgements: We acknowledge William Burhans for his encouragement and support, and grants from the National Institutes of Health: R21ES1954, F33ES021133, and R15ES023685-03. We would like to thank Chris Vulpe for his gift of the pooled BY4743 library and guidance, Mingseng Sun for initiating work on AFB_1-induced recombination, Jonathan Bard for bioinformatics expertise, and Brian Kellner for technical contributions.

Figure Legends:

Figure 1: Expression of CYP1A2 in the yeast diploid strain (BY4743). Top right indicates CYP1A2-mediated activation of AFB_1 to form a highly reactive epoxide that forms DNA, RNA, and protein adduct. The lower left panel is a Western blot indicating 75, 50 and 37 kDa molecular weight markers. Lanes A and B are lysates from BY4743 and BY4743 cells expressing CYP1A2, respectively. The CYP1A2 (58 kDa) protein and the β-actin (42 kDa) protein are indicated. Right upper panel is a growth curve of the diploid wild type (BY4743) and BY4743 + pCS316 after exposure to 100 μM AFB. Right lower panel is a growth curve of BY4743 + pCS316 and *rad52* + pCS316 after exposure to 1% DMSO and 100 μM AFB_1. Growth (A_{600}) is plotted against time (Hs). Standard deviations are indicated at 1 h time points.

Figure 2: Growth curves for selected diploid mutants identified in the high throughput screen. A_{600} is plotted against time (Hs). Standard deviations are indicated at 1 h time points. The growth curves are indicated for wild type (BY4743) and *csm2*, *alk1*, *ssm4*, *cue1*, and *trm9*. The bar graph indicates area % growth of AFB_1-exposed strains as determined by ratio of the area under curves (area under the curve for treated strain/area under the curve for strain exposed to DMSO x 100%).

Figure 3. GO enrichment for the yeast genome compared to AFB_1 resistant genes, as performed by Panther analysis. The top circles represent the % genes of that are grouped according to Process. The bottom group are those which are grouped according to protein class. GO groups included post replication repair, response to

chemical, DNA repair, error-prone DNA synthesis, non-error prone DNA synthesis, and non-classified. Number of genes belonging to each GO is indicated within the pie.

Figure 4. The protein interactome encoded by AFB_1 resistance genes in budding yeast (left, A) and protein interactome encoded by their associated human homologs (right, B). The interactome was curated using String V11 (https://string-db.org, Szklarczyk et al., 2019), using a high confidence level of .8 and MCL cluster factor of 1.1. Proteins are represented by colored circles (nodes); different colors represent distinct interacting clusters. A core group, in red seen in both images, includes proteins that function in DNA repair pathways, and interact with proteases, transcription and cell cycle factors.. Lines represent the edges; a solid blue line indicates a binding event, a dark line indicates a reaction, and a purple line indicates catalysis. The lighter lines indicate a strong connection, as deduced from the literature. Lines that terminate with a dot indicate an unspecified interaction, whether positive or negative.

Figure 5. AFB_1-associated sister chromatid recombination and mutagenesis frequencies in the wild type and *csm2* haploid mutant. The top part of the panel shows the assays for sister chromatid exchange and mutagenesis; for both assays the oval represents the centromere and the single line represents duplex DNA. For simplicity, the left arm of chromosomes IV and V are not shown. (Top left) Unequal sister chromatid recombination is monitored by selecting for His^+ prototrophs that result from recombination between the juxtaposed, truncated *his3* fragments. The *his3*-Δ*3′* lacks the 3' sequences (arrow head), while the *his3*-Δ*5′* lacks to promoter sequences

(feathers). Both *his3* fragments are located with the amino acid reading frames oriented to the centromere. The *his3* fragments share a total of 450 bp sequence homology. (Top right). The mutation assay is measures the frequency of canavanine resistant mutants. The arrow notes the occurrence of point, missense, or deletion mutations that can occur in the *CAN1* gene.

Figure 6. Growth of wild type (BY4741), *csm2* , *rad4*, *rad51*, *csm2 rad51*, and *csm2 rad4* cells after exposure to 50 and 100 μM AFB_1. (Left) Growth of cells containing pCS316 and expressing CYP1A2 after chronic exposure to 0.5% and 1.0% DMSO (black), 50 *μ*M (red), and 100 *μ*M (red) AFB_1. The relevant genotype is given above the panel (see Table 1, for complete genotype). Approximately 10^5 log-phase cells were inoculated in each well, n = 2. A_{600} is plotted against time (hs). Bars indicate the standard deviations of measurements, n = 2.

Supplemental Figure 1. Percent growth calculated by area under the curves (AUCs) for yeast strains containing designated deletions after exposure to 50 μM AFB and/or 100 μM AFB. Panel A: Percent growth calculated for specific deletion strains after exposure to 50 μM AFB. Panel B: Percent growth calculated for specific strains after exposure to 50 μM AFB and/or 100 μM AFB. Percent growth were calculated by determining the ratio of the AUC after exposure to toxin to the AUC exposed to solvent (dimethyl sulfoxide) alone.

Supplemental Figure 2. Growth curve of the diploid wild type (BY4743 + pCS316), *shu1* + pCS316, *shu2* + pCS316, and *psy3* + pCS316 after exposure to 50 μM AFB. Growth (A_{600}) is plotted against time (Hs). Standard deviations are indicated at 1 h time points, n = 2. See supplemental figure 1 for percent growth.

LITERATURE CITED

Aggarwal M., and R. Brosh, 2012 Functional analyses of human DNA repair proteins important for aging and genomic stability using yeast genetics. DNA Repair (Amst). 11(4):335-438.

Alekseyev O., M.L. Hamm, and J.M. Essigman, 2004 Aflatoxin B1 formamidopyrimidine adducts are preferentially repaired by the nucleotide excision repair pathway in vivo. Carcinogenesis. 25(6):1045-1051.

Amici M., V. Cecarini, A. Pettinari, L. Bonfili, M. Angeletti, et al., 2007 Binding of aflatoxins to the 20S proteasome: effects on enzyme functionality and implications for oxidative stress and apoptosis. Biol Chem. 388(1):107-117.

Ausubel F., R. Brent, R. Kingston, D. Moore, J. Seidman, J. Smith, K. Struhl, Current Protocols in Molecular Biology, Volume 1. Wiley and Sons, Inc., 1994.

Baertschi S.W., K.D. Raney, M.P. Stone, T.M. Harris, 1988 Preparation of the 8,9-Epoxide of the Mycotoxin Aflatoxin B1: The Ultimate Carcinogenic Species. J. Am. Chem. SOC 110:7929-793.

Barski O.A., S.M. Tipparaju, A. Bhatnagar, 2008 The aldo-keto reductase superfamily and

its role in drug metabolism and detoxification. Drug Metab Rev.40(4):553-624.

Barz T., K. Ackermann, G. Dubois, R. Eils, W. Pyerin, 2003 Genome-wide expression screens indicate a global role for protein kinase CK2 in chromatin remodeling. J Cell Sci.116(8):1563-77.

Bassler J., I. Klein, C. Schmidt, M. Kallas, E. Thomson, M.A. Wagner, B. Bradatsch, G. Rechberger, H. Strohmaier, E. Hurt, and H. Bergler, 2012 The conserved Bud20 zinc finger protein is a new component of the ribosomal 60S subunit export machinery. Mol Cell Biol. 32(24):4898-4912. doi: 10.1128/MCB.00910-12.

Bedard L.L., and T.E. Massey, 2006 Aflatoxin B1-induced DNA damage and its repair. Cancer Lett. 241(2):174-183.

Begley U., M. Dyavaiah, A. Patil, J.P. Rooney, D. DiRenzo, C.M. Young, D.S. Conklin, R.S. Zitomer, T.J. Begley, 2007 Trm9-catalyzed tRNA modifications link translation to the DNA damage response. Mol Cell.14;28(5):860-870.

Bernabucci U., L. Colavecchia, P.P. Danieli, Ã. Basiric, N. Lacetera, A. Nardone, B. Ronchi, Aflatoxin B1 and fumonisin B1 affect the oxidative status of bovine peripheral blood mononuclear cells, In Toxicology in Vitro, Volume 25, Issue 3, 2011, Pages 684-691, ISSN 0887-2333, https://doi.org/10.1016/j.tiv.2011.01.009.

Bernstein K.A., R.J. Reid, I. Sunjevaric, K. Demuth, R.C. Burgess, and R. Rothstein. 2011 The Shu complex, which contains Rad51 paralogues, promotes DNA repair through inhibition of the Srs2 anti-recombinase. Mol Biol Cell. 22(9):1599-1607.

Birrell G.W., J.A. Brown, H.I. Wu, G. Giaever, A.M., Chu, R.W. Davis, and J.M. Brown, 2002 Transcriptional response of Saccharomyces cerevisiae to DNA-damaging agents does not identify the genes that protect against these agents. Proc Natl Acad Sci U S A. 99(13):8778-8783.

Brachmann C.B., et al., 1998 Designer deletion strains derived from *Saccharomyces cerevisiae* S288C: a useful set of strains and plasmids for PCR-mediated gene disruption and other applications. Yeast 14(2):115-132.

Brown, K.L., J.Z. Deng, I. Rajkumar, L.G. Iyer, M.W. Voehler, M.P. Stone, C.M. Harris, and T.M. Harris**,** 2006 Unraveling the Aflatoxin−FAPY Conundrum: Structural Basis for Differential Replicative Processing of Isomeric Forms of the Formamidopyrimidine-Type DNA Adduct of Aflatoxin B1. J. American Chem. Soc. 128 (47):15188-15199.

Brown R.L., Z.Y Chen., M Warburton., M. Luo, A Menkir, A Fakhoury., D Bhatnagar, 2010 Discovery and characterization of proteins associated with aflatoxin-resistance: evaluating their potential as breeding markers. Toxins (Basel). 2(4):919-33.

Burke D., D. Dawson, T. Stearns, 2000 Methods in yeast genetics, in: A Cold Spring Harbor Laboratory Course Manual, Cold Spring Harbor Press, New York.

Chawanthayatham S, C.C. Valentine, B.I. Fedeles, E.J. Fox, L.A. Loeb, S.S. Levine, S.L. Slocum, G.N. Wogan, R.G. Croy, J.M. Essigmann, 2017 Mutational spectra of aflatoxin B(1) in vivo establish biomarkers of exposure for human hepatocellular carcinoma. Proc. Natl. Acad. Sci. U S A. 114(15):3101-3109.

Cherry J.M., E.L. Hong, C. Amundsen, R. Balakrishnan, G. Binkley, E.T. Chan, K.R. Christie, M.C. Costanzo, S.S. Dwight, S.R. Engel, D.G. Fisk, J.E. Hirschman, B.C. Hitz, K. Karra, C.J. Krieger, S.R. Miyasato, R.S. Nash, J. Park, M.S. Skrzypek, M. Simison, S. Weng, and E.D. Wong, 2012 Saccharomyces Genome Database: the genomics resource of budding yeast. Nucleic Acids Res. 40(Database issue):D700-5.

Cheung W.L., F.B. Turner, T. Krishnamoorthy, B. Wolner, S.H. Ahn, M. Foley, J.A. Dorsey
C.L. Peterson, S.L. Berger, and C.D. Allis, 2005 Phosphorylation of histone H4 serine 1 during DNA damage requires casein kinase II in S. cerevisiae. Curr Biol.15(7):656-660. PMID: 15823538.

Chua M.M., C.E. Ortega, A. Sheikh, M. Lee, H. Abdul-Rassoul, K.L. Hartshorn, and I. Dominguez, 2017 CK2 in Cancer: Cellular and Biochemical Mechanisms and Potential Therapeutic Target. Pharmaceuticals (Basel). 10(1). pii: E18.

Crespi C.L., B.W. Penman, D.T. Steimel, H.V. Gelboin, F.J. Gonzalez, 1991 The development of a human cell line stably expressing human CYP3A4: role in the metabolic activation of aflatoxin B1 and comparison to CYP1A2 and CYP2A3. Carcinogenesis12(2):355-359.

Croy R.G., and G.N. Wogan, 1981 Temporal patterns of covalent DNA adducts in rat liver
after single and multiple doses of aflatoxin B1. Cancer Res. 41(1):197-203.

Dancis A, et al. 1994 The Saccharomyces cerevisiae copper transport protein (Ctr1p). Biochemical characterization, regulation by copper, and physiologic role in copper uptake. J. Biol. Chem. 269(41):25660-7.

De La Rosa, V.Y., J. Asfaha, M. Fasullo**,** A. Loguinov, P. Li, J. Nakamura, J.Swenberg, M. T. Smith, C. Vulpe, D.G. Scelo, 2017 Functional profiling in yeast reveals genotoxicity mechanisms and candidate susceptibility genes associated with trichloroethylene exposure and renal cell carcinoma. Toxicol Sci. 160(1):111-120.

De Mattia E., E. Cecchin, J. Polesel, A. Bignucolo, R. Roncato, F. Lupo, M. Crovatto, A. Buonadonna, C. Tiribelli, G. Toffoli, 2017 Genetic biomarkers for hepatocellular cancer risk in a caucasian population. World J Gastroenterol. 23(36):6674-6684.

Dhont L., C. Mascaux, A. Belayew, 2016 The helicase-like transcription factor (HLTF) in cancer: loss of function or oncomorphic conversion of a tumor suppressor? Cell Mol Life Sci. 73(1):129-147.

Dotan I., E. Ziv, N. Dafni, J.S. Beckman, R.O. McCann, C.V. Glover, D. Canaani, 2001 Functional conservation between the human, nematode, and yeast CK2 cell cycle genes. Biochem Biophys Res Commun. 288(3):603-609.

Dong Z., and M. Fasullo 2003 Multiple recombination pathways for sister chromatid exchange in Saccharomyces cerevisiae: role of RAD1 and the RAD52 epistasis group genes. Nucleic Acids Res. 31(10):2576-2585.

Eaton D.L., and E.P. Gallagher,1994 Mechanisms of aflatoxin carcinogenesis. Ann. Rev. Pharmacol. Toxicol., 34:135-172.

Essigmann, J.M., R.G. Croy, A.M. Nadzan, W.F. Busby, V.N. Reinhold, G. Buchi, and G.N. Wogan, 1977 Structural identification of the major DNA adduct formed by aflatoxin B1 in vitro. Proc. Natl. Acad. Sci. USA, 74: 1870-1874.

Eugster H.P., S. Bärtsch, F.E. Würgler, and C. Sengstag, 1992 Functional co-expression of human oxidoreductase and cytochrome P450 1A1 in Saccharomyces cerevisiae results in increased EROD activity. Biochem Biophys Res Commun. 185: 641-647.

Fasullo M.T., and R.W. Davis, 1987. Recombinational substrates designed to study recombination between unique and repetitive sequences in vivo. Proc Natl Acad Sci U S A. 84(17):6215-9.

Fasullo M, Chen Y, Bortcosh W, Sun M, Egner PA, 2010. Aflatoxin B(1)-Associated DNA
Adducts Stall S Phase and Stimulate Rad51 foci in Saccharomyces cerevisiae. J. Nucleic Acids. 1:456487.

Fasullo M., M. Sun, and P. Egner, 2008 Stimulation of sister chromatid exchanges and mutation by aflatoxin B1-DNA adducts in Saccharomyces cerevisiae requires MEC1 (ATR), RAD53, and DUN1. Mol Carcinog. 47(8):608-615.

Fasullo M., A. Smith, P. Egner, C. Cera, 2014 Activation of aflatoxin B1 by expression of human CYP1A2 polymorphisms in Saccharomyces cerevisiae. Mutat. Res. Genet. Toxicol. Environ. Mutagen. 761:18-26.

Fasullo M.T., and M. Sun, Both RAD5-dependent and independent pathways are involved
in DNA damage-associated sister chromatid exchange in budding yeast. AIMS Genet. 2017;4(2):84-102. doi: 10.3934/genet.2017.2.84.

Foiani, M., F. Marini, D. Gamba, G. Lucchini, P. Plevani,1994 The β subunit of the DNA polymerase alpha-primase complex in *Saccharomyces cerevisiae* executes an essential function at the initial stage of DNA replication. Mol. Cell Biol. 14(): 923–933.

Furukawa T., M. Komatsu, R. Ikeda, K. Tsujikawa, and S.Akiyama, 2008. Copper transport systems are involved in multidrug resistance and drug transport. Curr Med Chem. 15(30):3268-3278.

Giaever G., A.M. Chu, L. Ni, C. Connelly, L. Riles, S. Véronneau, et al., 2002 Functional profiling of the Saccharomyces cerevisiae genome. Nature. 418(6896):387-391.

Giaever G, P. Flaherty, J. Kumm, M. Proctor, C. Nislow, D.F. Jaramillo, A.M. Chu, M.I. Jordan, A.P. Arkin, and R.W. Davis, 2004. Chemogenomic profiling. Proc Natl Acad Sci U S A. 101(3):793-798.

Giaever, G., and C. Nislow, 2014 The yeast deletion collection: a decade of functional genomics. Genetics 197: 451–465.

Gray GK, McFarland BC, Rowse AL, Gibson SA, Benveniste EN. Therapeutic CK2 inhibition attenuates diverse prosurvival signaling cascades and decreases cell viability in human breast cancer cells. Oncotarget. 2014 Aug 15;5(15):6484-96.

Greetham D., and C.M. Grant, 2009 Antioxidant activity of the yeast mitochondrial one-Cys peroxiredoxin is dependent on thioredoxin reductase and glutathione in vivo. Mol. Cell Biol. 29(11):3229-3240

Gietz R.D., and R.H. Schiestl, 2007. Microtiter plate transformation using the LiAc/SS carrier DNA/PEG method. Nat Protoc. 2(1):5-8.

Gallagher E.P., K.L. Kunze, P.L. Stapleton, and D.L. Eaton, 1996 The kinetics of aflatoxin B1 oxidation by human cDNA-expressed and human liver microsomal cytochromes P450 1A2and 3A4**.** Toxicol. Appl. Pharmacol. 141:(2) 595–606.

Glassner B.J., and R.K. Mortimer, 1994. Synergistic interactions between *RAD5*, *RAD16* and
RAD54, three partially homologous yeast DNA repair genes each in a different repair pathway. Radiat Res. 139(1):24-33.

Godin S.K., Z. Zhang, B.W. Herken, J.W. Westmoreland, A.G. Lee, M.J. Mihalevic, Z. Yu,
R.W. Sobol, M.A. Resnick, K.A. Bernstein, 2016 The Shu complex promotes error-free tolerance of alkylation-induced base excision repair products. Nucleic Acids Res. 44(17):8199-8215.

Guillemain G., E. Ma, S. Mauger, S. Miron, R. Thai, R. Guérois, F. Ochsenbein,

And M.C. Marsolier-Kergoat, 2007 Mechanisms of checkpoint kinase Rad53 inactivation after a double-strand break in Saccharomyces cerevisiae. Mol Cell Biol. 27(9):3378-89.

Guo Y, L.L. Breeden, H. Zarbl, B.D. Preston, and D.L. Eaton, 2005 Expression of a human cytochrome p450 in yeast permits analysis of pathways for response to and repair of aflatoxin-induced DNA damage. Mol Cell Biol. 25(14):5823-5833.

Guo Y, L.L. Breeden, W. Fan, L.P. Zhao, D.L. Eaton, H. Zarbl, 2006 Analysis of cellular responses to aflatoxin B(1) in yeast expressing human cytochrome P450 1A2 using cDNA microarrays. Mutat Res. 29;593(1-2):121-42.

Herbert G.B., B. Shi, and R.B. Gartenhaus, 2001 Expression and stabilization of the MCT-1 protein by DNA damaging agents. Oncogene. 20(46):6777-6783.

Hoffman C.S., and F. Winston. 1987 A ten-minute DNA preparation from yeast efficiently releases autonomous plasmids for transformation of Escherichia coli. Gene 57:267–272.

Hsu I.C., R.A. Metcalf, T. Sun, J.A. Welsh, N.J. Wang, and C.C. Harris, 1991 Mutational hotspot in the p53 gene in human hepatocellular carcinomas. Nature 350: 427-428.

Hsu H.L., C.O. Choy, R. Kasiappan, H.J. Shih, J.R. Sawyer, C.L. Shu, K.L. Chu, Y.R.Chen, H.F. Hsu, and R.B. Gartenhaus, 2007 MCT-1 oncogene downregulates p53

and destabilizes genome structure in the response to DNA double-strand damage. DNA Repair (Amst). 1;6(9):1319-1332.

Huang M.N., W. Yu, W.W. Teoh, M. Ardin, A. Jusakul, A.W. Ng, A. Boot, B. Abedi-Ardekani, S. Villar, S.S. Myint, R. Othman, S.L. Poon, A. Heguy, M. Olivier, M. Hollstein, P. Tan, B.T. Teh, K. Sabapathy, J. Zavadil, S.G. Rozen, 2017. Genome-scale mutational signatures of aflatoxin in cells, mice, and human tumors. Genome Res. 27(9):1475-1486.

Ji R.B., Y.S. Qian, A.R. Hu, and Y.R. Hu, 2015 DNA repair gene XRCC3 T241M polymorphism and susceptibility to hepatocellular carcinoma in a Chinese population: a meta-analysis. Genet Mol Res. 14(4):15988-15996.

Jo W.J., A. Loguinov, H. Wintz, M. Chang, A.H. Smith, D. Kalman, L. Zhang, M.T. Smith,
C.D. Vulpe, 2009. Comparative functional genomic analysis identifies distinct and overlapping sets of genes required for resistance to monomethylarsonous acid (MMAIII) and arsenite (AsIII) in yeast. Toxicol Sci. 111(2):424-436.

Kachroo A.H., J.M. Laurent, C.M. Yellman, A.G. Meyer, C.O. Wilke, and E.M. Marcotte, 2015 Evolution. Systematic humanization of yeast genes reveals conserved functions and genetic modularity. Science 348(6237):921-925.

Kanaar R., C. Troelstra, S.M. Swagemakers, J. Essers, B. Smit, J.H. Franssen, A. Pastink, O.Y. Bezzubova, J.M. Buerstedde, B. Clever, W.D. Heyer, J.H. Hoeijmakers, 1996 Human and
mouse homologs of the Saccharomyces cerevisiae RAD54 DNA repair gene: evidence for functional conservation. Curr Biol. 6(7):828-838.

Kasiappan R., H.J. Shih, K.L. Chu, W.T. Chen, H.P. Liu, S.F. Huang, C.O. Choy, C.L. Shu, R. Din, J.S. Chu, and H.L. Hsu, 2009. Loss of p53 and MCT-1 overexpression synergistically promotechromosome instability and tumorigenicity. Mol. Cancer Res. 7(4):536-548.

Keller-Seitz, M., U. Certa, C. Sengstag, F. Wurgler, M. Sun, and M. Fasullo, 2004 Transcriptional response of the yeast to the carcinogen Aflatoxin B1: Recombinational repair involving *RAD51* and *RAD1*. Mol. Biol. Cell. 15:4321-4336.

Leadon S.A., R.M. Tyrrell, and P.A. Cerutti, 1981 Excision repair of aflatoxin B1-DNA adducts in human fibroblasts. Cancer Res. 41(12 Pt 1):5125-5129.

Lee W., RP St Onge, M Proctor, P Flaherty, MI Jordan, AP Arkin, RW Davis, C Nislow, and G.Giaever, 2005. Genome-wide requirements for resistance to functionally distinct DNA-damaging agents. PLoS Genet. 1(2):e24.

Li L., S. Miles, and L.L. Breeden LL, 2015 A Genetic Screen for Saccharomyces cerevisiae Mutants That Fail to Enter Quiescence. G3 (Bethesda). 5(8):1783-1795.

Li Q., K. Li, T. Yang, S. Zhang, Y. Zhou, Z. Li, J. Xiong, F. Zhou, X. Zhou, L. Liu, R. Meng, and G. Wu, 2017 Association of protein kinase CK2 inhibition with cellular radiosensitivity of non-small cell lung cancer. Sci Rep.;7(1):16134.

Lin Y.C., L. Li, A.V. Makarova, P.M. Burgers, M.P. Stone, and R.S. Lloyd RS, 2014 Error-prone replication bypass of the primary aflatoxin B1 DNA adduct, AFB_1-N7-Gua. J. Biol. Chem. 289(26):18497-18506..

Lin,J.-K., J.A. Miller, and E.C Miller, 1977 2,3-Dihydro-2-(guan-7-yl)-3-hydroxy-aflatoxin B1, a major acid hydrolysis product of aflatoxin B1-DNA or -ribosomal RNA adducts formed in hepatic microsome-mediated reactions in rat liver in vivo. Cancer Res., 37:4430-4438.

Liu, Y., W. Wang, 2016 Aflatoxin B1 impairs mitochondrial functions, activates ROS generation, induces apoptosis and involves Nrf2 signal pathway in primary broiler hepatocytes. Anim. Sci. J. 87:1490–1500.

Long X.D., J.G. Yao, Z. Zeng, Y. Ma, X.Y. Huang, *et al.*, 2013 Polymorphisms in the coding region of X-ray repair complementing group 4 and aflatoxin B1-related hepatocellular carcinoma. Hepatology. 58(1):171-181.

Long X.D, Y. Ma, D.Y. Qu, Y.G. Liu, Z.Q. Huang, 2008 The Polymorphism of XRCC3 codon 241 and AFB_1-related hepatocellular carcinoma in Guangxi population, China. Ann Epidemiol. 18(7):572-578.

Merrick B.A., D.P. Phadke, S.S. Auerbach, D. Mav, S.M Stiegelmeyer, R.R. Shah, R.R Tice, 2013 RNA-Seq profiling reveals novel hepatic gene expression pattern in aflatoxin B1 treated rats. PLoS One. 8(4):e61768

Mi H., X. Huang, A. Muruganujan, H. Tang, , C. Mills, D. Kang, , P.D. Thomas, 2016 PANTHER version 11: expanded annotation data from Gene Ontology and Reactome pathways, and data analysis tool enhancements Nucl. Acids Res. 45(D1):D183-D189.

Martin, C.N. and R.C. Garner, 1977 Aflatoxin B1-oxide generated by chemical or enzymatic oxidation of aflatoxin B1 causes guanine substitution in nucleic acids. Nature 267:863-865.

Mary V.S., M.G. Theumer, S.L. Arias, H.R. Rubinstein, 2012. Reactive oxygen species sources
and biomolecular oxidative damage induced by aflatoxin B1 and fumonisin B1 in rat spleen mononuclear cells. Toxicology 302(2-3):299-307.

Murray B.P., and M.A. Correia, 2001 Ubiquitin-dependent 26S proteasomal pathway: a role in the degradation of native human liver CYP3A4 expressed in Saccharomyces cerevisiae? Arch Biochem Biophys. 393(1):106-116.

O'Connor S.T., et al., 2012 Genome-Wide Functional and Stress Response Profiling Reveals Toxic Mechanism and Genes Required for Tolerance to Benzo[a]pyrene in S. cerevisiae. Front Genet 3:316.

Pan H.Z., J. Liang, Z. Yu, L.M. Lun, H. Li, and Q. Wang, 2011 Polymorphism of DNA repair gene XRCC1 and hepatocellular carcinoma risk in Chinese population. Asian Pac J Cancer Prev. 12(11):2947-2950.

Pereyra C., L. Cavaglieri, S. Chiacchiera, and A. Dalcero, 2013 The corn influence on the adsorption levels of aflatoxin B_1 and zearalenone by yeast cell wall. J Appl Microbiol, 114: 655-662.

Perugorria M.J., J.M.Banales, 2017 Genetics: Novel causative genes for polycystic liver disease. Nat Rev Gastroenterol Hepatol. 14(7):391-392.

Pierce S.E., E.L. Fung, D.F. Jaramillo, A.M. Chu, R.W. Davis, C. Nislow, G. Giaever, 2006 A unique and universal molecular barcode array. Nat Methods. 3(8):601-603.

Pompon, D., B. Louerat, A. Bronine, and P. Urban, 1996 Yeast expression of animal and plant P450s in optimized redox environments. Methods Enzymol. 272: 51-64

Porath B., V.G Gainullin., E Cornec-Le Gall., E.K Dillinger., C.M Heyer., K Hopp., M.E.Edwards, C.D.Madsen, S.R Mauritz., C.J.,Banks, et. al., 2016. Mutations in GANAB, Encoding the Glucosidase IIα Subunit, Cause Autosomal-Dominant Polycystic Kidney and Liver
Disease. Am J Hum Genet. 98(6):1193-1207.

Robinson M.D., D.J. McCarthy, and G.K. Smyth, 2010 edgeR: a Bioconductor package for differential expression analysis of digital gene expression data. Bioinformatics. 26(1):139-140..

Robinson M.D., and A. Oshlack, 2010 A scaling normalization method for differential expression analysis of RNA-seq data. Genome Biol. 11(3):R25.

Said M.R., T.J. Begley, A.V. Oppenheim, D.A. Lauffenburger, L.D. Samson, 2004 Global network analysis of phenotypic effects: protein networks and toxicity modulation in
Saccharomyces cerevisiae. Proc Natl Acad Sci U. S. A. 101(52):18006-18011.

Schonbrun M., M. Kolesnikov, M. Kupiec, R. Weisman, 2013 TORC2 is required to maintain

genome stability during S phase in fission yeast. J Biol Chem. 288(27):19649-19660.

Schmidt A, et al., 1996 TOR2 is required for organization of the actin cytoskeleton in yeast. Proc Natl Acad Sci U S A 93(24):13780-13785.

Sengstag C, H.P. Eugster, and F.E. Wurgler, 1994 High promutagen activating capacity of yeast microsomes containing human cytochrome P-450 1A and human NADPH-cytochrome P-450 reductase. Carcinogenesis. 15(5):837-843.

Sengstag C., B. Weibel, and M. Fasullo, 1996 Genotoxicity of aflatoxin B1: Evidence for a recombination-mediated mechanism in Saccharomyces cerevisiae. Cancer Research 56:5457-5465.

Shen H.M, C.N. Ong, and C.Y. Shi,1995 Involvement of reactive oxygen species in aflatoxin B1-induced cell injury in cultured rat hepatocytes. Toxicology 99(1-2):115-123.

Shen H.M., and C.N. Ong, 1996, Mutations of the p53 tumor suppressor gene and ras oncogenes in aflatoxin hepatocarcinogenesis. Mutat. Res. Rev. Genet. Toxicol. 366:23-44.

Shimada K., I. Filipuzzi, M. Stahl, S.B. Helliwell, C. Studer, D. Hoepfner, A. Seeber, R. Loewith, N.R. Movva, S.M. Gasser, 2013. TORC2 signaling pathway guarantees genome

stability in the face of DNA strand breaks. Mol Cell. 51(6):829-39.

Shinohara A., H. Ogawa and T. Ogawa, 1992 Rad51 protein involved in repair and recombination in S. cerevisiae is a RecA like protein. Cell 69: 457–470.

Shor E., J. Weinstein, R. Rothstein, 2005 A genetic screen for top3 suppressors in Saccharomyces cerevisiae identifies SHU1, SHU2, PSY3 and CSM2: four genes involved in error-free DNA repair. Genetics 169(3):1275-89.

Singh, K.B., B.K.Maurya, and S.K. Trigun, 2015 Activation of oxidative stress and inflammatory factors could account for histopathological progression of aflatoxin-B1 induced hepatocarcinogenesis in rat. Mol. Cell Biochem. 401:185.

Smela M.E., M..L Hamm, P.T. Henderson, C.M. Harris, T.M. Harris, J.M. Essigmann,2002 The aflatoxin B(1) formamidopyrimidine adduct plays a major role in causing the types of mutations observed in human hepatocellular carcinoma. Proc Natl Acad Sci U S A.99(10):6655-60.

Smith A.M., L.E. Heisler, R.P, St Onge, E,Farias-Hesson, I.M. Wallace, J, Bodeau A.N. Harris, K.M. Perry, G. Giaever, N. Pourmand, C. Nislow,. 2010 Highly-multiplexed barcode sequencing: an efficient method for parallel analysis of pooled samples. Nucleic Acids Res. 38(13):e142.

St Onge R.P., R. Mani, J. Oh, M. Proctor, E. Fung, R.W. Davis, C. Nislow, F.P. Roth, G.Giaever, 2007 Systematic pathway analysis using high-resolution fitness profiling of combinatorial gene deletions. Nat Genet. 39(2):199-206.

Sun J., T. Nishiyama, K. Shimizu, K. Kadota, 2013 TCC: an R package for comparing tag count data with robust normalization strategies. BMC Bioinformatics. 2013 9;14:219.

Szklarczyk D., A.L. Gable, D. Lyon, A. Junge, S. Wyder, J. Huerta-Cepas, M. Simonovic, N.T. Doncheva, J.H. Morris, P. Bork, L.J. Jensen, C. von Mering, 2019 STRING v11: protein-protein association networks with increased coverage, supporting functional discovery in genome-wide experimental datasets**.** Nucleic Acids Res. 47:607-613.

Tkach J.M., A. Yimit, A.Y. Lee, M. Riffle, M. Costanzo, D. Jaschob, J.A. Hendry, J. Ou, J. Moffat, C. Boone, T.N. Davis, C. Nislow, G.W. Brown, 2012 Dissecting DNA damage response pathways by analyzing protein localization and abundance changes during DNA replication stress. Nat. Cell Biol. 14(9):966-976.

Toczyski D.P., D.J. Galgoczy, L.H. Hartwell, 1997 CDC5 and CKII control adaptation to the yeast DNA damage checkpoint. Cell. 90(6):1097-1106.

Trembley J.H., B.T. Kren, M.J. Abedin, R.I. Vogel, C.M. Cannon, G.M. Unger, K. Ahmed, 2017 CK2 Molecular Targeting-Tumor Cell-Specific Delivery of RNAi in Various Models of
Cancer. Pharmaceuticals (Basel).10(1). pii: E25.

Unk I., I.Hajdú, and A. Blastyák, et al., 2010 Role of yeast Rad5 and its human orthologs, HLTF and SHPRH in DNA damage tolerance. DNA Repair. 9:257–267.

Van Leeuwen S., P.E. Jolanda, N. Vermeulen, C. Vos, J., 2012 Current Drug Metabolism 13 (10):1464-1475

Vartanian V., I.G.Minko, S.Chawanthayatham, P.A.Egner, Y.C.Lin, L.F.Earley, R.Makar, J.R.Eng, M.T.Camp, L.Li, M.P.Stone, M.R. Lasarev, J.D.Groopman, R.G.Croy, J.M. Essigmann, A.K McCullough., R.S.Lloyd, 2017 NEIL1 protects against aflatoxin-induced hepatocellular carcinoma in mice. Proc Natl Acad Sci U S A. 114(16):4207-4212.

Weng M.W., H.W.Lee, B.Choi, H.T.Wang, Y.Hu, M.Mehta, D.Desai, S.Amin, Y.Zheng, M.S.Tang, 2017 AFB_1 hepatocarcinogenesis is via lipid peroxidation that inhibits DNA repair, sensitizes mutation susceptibility and induces aldehyde-DNA adducts at p53 mutational hotspot codon 249. Oncotarget. 8(11):18213-18226. doi:10.18632/oncotarget.15313.

Xu W., S.A.Liu, L.Li, Z.Y.Shen, and Y.L.Wu, 2015 Association between XRCC1 Arg280His polymorphism and risk of hepatocellular carcinoma: a systematic review and meta-analysis. Genet. Mol. Res. 14(2):7122-7129.

Xu X., L.Ball, W.Chen, X.Tian, A.Lambrecht, M.Hanna, and W. Xiao, 2013 The yeast Shu complex utilizes homologous recombination machinery for error-free lesion bypass via physical interaction with a Rad51 paralogue. PLoS One. 8(12):e81371..

Zhang X, H.M. Li, Z. Liu, G. Zhou, Q. Zhang, T. Zhang, J. Zhang, C. Zhang, 2013. Loss of heterozygosity and methylation of multiple tumor suppressor genes on chromosome 3 in hepatocellular carcinoma. J Gastroenterol. 48(1):132-143.

Zhang H.X., S.S. Jiang, X.F. Zhang, Z.Q. Zhou, Q.Z. Pan, C.L.Chen, J.J. Zhao, Y.Tang, J.C. Xia, and D.S Weng, 2015. Protein kinase CK2α catalytic subunit is overexpressed and serves as an unfavorable prognostic marker in primary hepatocellular carcinoma. Oncotarget. 6(33):34800-34817.

Zhou B., and J. Gitschier, 1997 h*CTR1*: A human gene for copper uptake identified by complementation in yeast. Proc. Natl. Acad. Sci. U.S.A. 94 (14) 7481-7486.

Zhou C., F. Bi, J. Yuan, F. Yang, S. Sun, 2018 Gain of UBE2D1 facilitates hepatocellular carcinoma progression and is associated with DNA damage caused by continuous IL-6. J Exp Clin Cancer Res. 27;37(1):290.

Table 1. Fitness Scores for 15 AFB_1 Resistant Genes Related to DNA Repair and Ranked by Significance

Gene[1.]	m. value[2.]	Gene Function	q.value[3.]
RAD54	-6.60183	DNA-dependent ATPase that stimulates strand exchange; modifies the topology of double-stranded DNA; involved in the recombinational repair of double-strand breaks in DNA during vegetative growth and meiosis; member of the SWI/SNF family of DNA translocases; forms nuclear foci upon DNA replication stress	3.09E-13
*RAD2**	-3.72604	Single-stranded DNA endonuclease; cleaves single-stranded DNA during nucleotide excision repair to excise damaged	1.03E-10
*RAD55***	-3.97622	Protein that stimulates strand exchange; stimulates strand exchange by stabilizing the binding of Rad51p to single-stranded DNA	1.96E-07
REV3	-4.15215	Catalytic subunit of DNA polymerase zeta	2.39E-07
RAD10	-2.34872	Single-stranded DNA endonuclease (with Rad1p); cleaves single-stranded DNA during nucleotide excision repair and double-strand break repair	3.04E-07
REV1	-4.06683	Deoxycytidyl transferase	4.89E-06
RAD17	-4.23719	Checkpoint protein; involved in the activation of the DNA damage and meiotic pachytene checkpoints; with Mec3p and Ddc1p, forms a clamp that is loaded onto partial duplex DN	9.13E-06
NUP60	-2.48861	FG-nucleoporin component of central core of the nuclear pore complex; contributes directly to nucleocytoplasmic transport and maintenance of the nuclear pore complex (NPC) permeability barrier and is involved in gene tethering at the nuclear periphery; relocalizes to the cytosol in response to hypoxia	0.000118
*RAD18***	-3.30101	E3 ubiquitin ligase; forms heterodimer with Rad6p to monoubiquitinate PCNA-K164	0.004213
RAD23	-6.20456	Protein with ubiquitin-like N terminus; subunit of Nuclear Excision Repair Factor 2 (NEF2) with Rad4p that binds damaged DNA; enhances protein deglycosylation activity of Png1p; also involved, with Rad4p, in ubiquitylated protein turnover; Rad4p-Rad23p heterodimer binds to promoters of DNA damage response genes to repress their transcription in the absence of DNA damage	0.018765
*RAD4**	-	Protein that recognizes and binds damaged DNA (with	0.049856

	2.22301	Rad23p) during NER; subunit of Nuclear Excision Repair	
*RAD1**	-5.42906	Single-stranded DNA endonuclease (with Rad10p); cleaves single-stranded DNA during nucleotide excision repair and double-strand break repair; subunit of Nucleotide Excision Repair Factor 1 (NEF1); homolog of human XPF protein [2] [3] [4]	0.061213
RAD5*	-3.79042	DNA helicase/Ubiquitin ligase; involved in error-free DNA damage tolerance (DDT), replication fork regression during postreplication repair by template switching, error-prone translesion synthesis	0.06955
CSM2	-1.25308	Component of Shu complex (aka PCSS complex); Shu complex also includes Psy3, Shu1, Shu2, and promotes error-free DNA repair	0.079022
PSY3	-2.11872	Component of Shu complex (aka PCSS complex); Shu complex also includes Shu1, Csm2, Shu2, and promotes error-free DNA repair; promotes Rad51p filament assembly	0.092629

[1.] Genes in bold encode proteins whose cellular locations are affected by DNA replication stress, *Appears Twice Among Screens ($q < 0.1$),**Appears Twice Among Screens ($q < 0.1$ and $p < 0.05$)

[2.] m.value is the numeric vector of fold change on a log2 scale

[3.] q value is the numeric vector calculated based on the p-value using the p.adjust function with default parameter settings.

Table 2. Fitness Scores for 70 AFB_1 resistant genes ranked by significance

Gene[1].	m. value[2].	Gene Function	q.value[3].
MIX23	-4.06328	Mitochondrial Intermembrane space CX(n)C motif protein	4.35E-10
MRPL35	-4.28367	Mitochondrial ribosomal protein of the large subunit	9.14E-10
BIT2	-3.96333	Subunit of TORC2 membrane-associated complex	1.47E-08
MNN10	-4.30245	Subunit of a Golgi mannosyltransferase complex	1.59E-08
YND1	-4.42756	Yeast Nucleoside Diphosphatase	2E-08
SPO1	-3.51771	Meiosis-specific prospore protein	5.48E-07
PYK2	-3.9434	Pyruvate kinase; appears to be modulated by phosphorylation	8.44E-07
TMA20	-3.17638	Protein of unknown function that associates with ribosomes; has a putative RNA binding domain; interacts with Tma22p; null mutant exhibits translation defects; has homology to human oncogene MCT1.	9.88E-07
DET1	-4.34985	Decreased Ergosterol Transport	2.06E-06
TRX3	-4.37389	Mitochondrial thioredoxin	2.62E-06
SSM4	-1.66932	Membrane-embedded ubiquitin-protein ligase; ER and inner nuclear membrane localized RING-CH domain E3 ligase involved in ER-associated protein degradation (ERAD)	5.11E-06
AKL1	-3.05176	Ser-Thr protein kinase; member (with Ark1p and Prk1p) of the Ark kinase family; involved in endocytosis and actin cytoskeleton organization	5.26E-06
PPG1	-2.78494	Putative serine/threonine protein phosphatase; putative phosphatase of the type 2A-like phosphatase family, required for glycogen accumulation	8.95E-05
GTB1	-2.67674	Glucosidase II beta subunit, forms a complex with alpha subunit Rot2p; involved in removal of two glucose residues from N-linked glycans during glycoprotein biogenesis in the ER; relocalizes from ER to cytoplasm upon DNA replication stress	8.95E-05
VPS13	-7.39394	Protein involved in prospore membrane morphogenesis; peripheral membrane protein that localizes to the prospore membrane and at numerous membrane contact sites; involved in sporulation, vacuolar protein sorting, prospore membrane formation	0.000118

		during sporulation, and protein-Golgi retention; required for mitochondrial integrity	
SVF1	-2.6069	Protein with a potential role in cell survival pathways; required for the diauxic growth shift; expression in mammalian cells increases survival under conditions inducing apoptosis	0.000253
ATP15	-3.45619	Epsilon subunit of the F1 sector of mitochondrial F1F0 ATP synthase	0.000292
TCM62	-4.00454	Protein involved in assembly of the succinate dehydrogenase complex; mitochondrial; putative chaperon	0.000432
SKG3	-2.79893	Protein of unknown function; green fluorescent protein (GFP)-fusion protein localizes to the cell periphery, cytoplasm, bud, and bud neck; potential Cdc28p substrate; similar to Skg4p; relocalizes from bud neck to cytoplasm upon DNA replication stress	0.000864
ATO3	-4.18208	Plasma membrane protein, putative ammonium transporter	0.000931
PET10	-7.89072	Protein of unknown function that localizes to lipid particles; large-scale protein-protein interaction data suggests a role in ATP/ADP exchange	0.001277
DAL82	-7.07535	Positive regulator involved in the degradation of allantoin	0.00347
PIB2	-5.64233	PhosphatidylInositol(3)-phosphate Binding	0.004213
DPB3	-2.15703	Third-largest subunit of DNA polymerase II (DNA polymerase epsilon); required to maintain fidelity of chromosomal replication and also for inheritance of telomeric silencing; stabilizes the interaction of Pol epsilon with primer-template DNA	0.004492
CKB1	-6.44401	Beta regulatory subunit of casein kinase 2 (CK2); a Ser/Thr protein kinase with roles in cell growth and proliferation; CK2, comprised of CKA1, CKA2, CKB1 and CKB2, has many substrates including transcription factors and all RNA polymerases	0.004492
RAV1	-5.1998	Regulator of (H+)-ATPase in Vacuolar membrane	0.004492
SWM1	-2.13536	Subunit of the anaphase-promoting complex (APC); APC is an E3 ubiquitin ligase that regulates the metaphase-anaphase transition and exit from mitosis	0.004492
GRE3	-2.09226	Aldose reductase; involved in methylglyoxal, d-xylose, arabinose, and galactose metabolism; stress induced (osmotic, ionic, oxidative, heat shock, starvation and heavy metals)	0.004492
HXK2	-2.0751	Hexokinase isoenzyme 2; phosphorylates glucose in	0.004492

		cytosol; predominant hexokinase during growth on glucose; represses expression of HXK1, GLK1	
PSY2	-5.27758	Subunit of protein phosphatase PP4 complex; Pph3p and Psy2p form the active complex, Psy4p may provide additional substrate specificity; regulates recovery from the DNA damage checkpoint, the gene conversion- and single-strand annealing-mediated pathways of meiotic double-strand break repair and efficient Non-Homologous End-Joining (NHEJ) pathway; Pph3p and Psy2p localize to foci on meiotic chromosomes; putative homolog of mammalian R3	0.006626
DIT1	-3.58127	Sporulation-specific enzyme required for spore wall maturation	0.006764
CKB2	-2.14702	Beta' regulatory subunit of casein kinase 2 (CK2); a Ser/Thr protein kinase with roles in cell growth and proliferation	0.010346
TES1	-1.9487	Peroxisomal acyl-CoA thioesterase	0.015718
MIS1	-1.7245	Mitochondrial C1-tetrahydrofolate synthase; involved in interconversion between different oxidation states of tetrahydrofolate (THF); provides activities of formyl-THF synthetase, methenyl-THF cyclohydrolase, and methylene-THF dehydrogenase	0.016405
ATP11	-1.86756	Molecular chaperone; required for the assembly of alpha and beta subunits into the F1 sector of mitochondrial F1F0 ATP synthase	0.019329
SCW10	-7.87538	Cell wall protein	0.019329
ROT2	-1.74496	Glucosidase II catalytic subunit; required to trim the final glucose in N-linked glycans; required for normal cell wall synthesis	0.019992
*FKH2***	-1.70355	Forkhead family transcription factor; rate-limiting activator of replication origins	0.020404
TRM9	-2.31801	tRNA methyltransferase; catalyzes modification of wobble bases in tRNA anticodons to 2, 5-methoxycarbonylmethyluridine and 5-methoxycarbonylmethyl-2-thiouridine; may act as part of a complex with Trm112p	0.022765
HHF1	-1.78433	Histone H4	0.026491
ATG29	-2.10149	Autophagy-specific protein; required for recruiting other ATG proteins to the pre-autophagosomal structure (PAS)	0.026491
MYO4	-1.7133	Type V myosin motor involved in actin-based transport of cargos	0.026491
PEX3	-2.0148	Peroxisomal membrane protein (PMP); required for proper localization and stability of PMP	0.03377

FUM1	-4.56102	Fumarase; converts fumaric acid to L-malic acid in the TCA cycle	0.03377
NRP1	-1.4818	Putative RNA binding protein of unknown function; localizes to stress granules induced by glucose deprivation; predicted to be involved in ribosome biogenesis	0.033997
*CUE1***	-1.09343	Ubiquitin-binding protein; ER membrane protein that recruits and integrates the ubiquitin-conjugating enzyme Ubc7p into ER membrane-bound ubiquitin ligase complexes that function in the ER-associated degradation (ERAD) pathway for misfolded proteins	0.037824
YIH1	-1.7379	Negative regulator of eIF2 kinase Gcn2p	0.040303
RPL9A	-1.63892	Ribosomal 60S subunit protein L9A; homologous to mammalian ribosomal protein L9 and bacterial L	0.044526
GLO1	-1.83782	Monomeric glyoxalase I; catalyzes the detoxification of methylglyoxal (a by-product of glycolysis) via condensation with glutathione to produce S-D-lactoylglutathione; expression regulated by methylglyoxal levels and osmotic stres	0.047337
CLB5	-1.74482	B-type cyclin involved in DNA replication during S phase	0.047457
*VOA1***	-6.41516	ER protein that functions in assembly of the V0 sector of V-ATPase; functions with other assembly factors; null mutation enhances the vacuolar ATPase (V-ATPase) deficiency of a vma21 mutant impaired in endoplasmic reticulum (ER) retrieval [1] [2]	0.049856
RPN10	-1.87723	Non-ATPase base subunit of the 19S RP of the 26S proteasome	0.053715
RPS4A	-1.65762	Protein component of the small (40S) ribosomal subunit; mutation affects 20S pre-rRNA processing; homologous to mammalian ribosomal protein S4	0.054912
RNR3	-1.3665	Minor isoform of large subunit of ribonucleotide-diphosphate reductase; the RNR complex catalyzes rate-limiting step in dNTP synthesis, regulated by DNA replication and DNA damage checkpoint pathways via localization of small subunit	0.056289
DST1	-1.88029	General transcription elongation factor TFIIS; enables RNA polymerase II to read through blocks to elongation by stimulating cleavage of nascent transcripts stalled at transcription arrest sites	0.05699
BCK2	-1.75834	Serine/threonine-rich protein involved in PKC1 signaling pathway; protein kinase C (PKC1) signaling pathway controls cell integrity; overproduction	0.06955

		suppresses pkc1 mutation	
BLM10	-1.5214	Proteasome activator; binds the core proteasome (CP) and stimulates proteasome-mediated protein degradation by inducing gate opening; required for sequestering CP into proteasome storage granule (PSG) during quiescent phase and for nuclear import of CP in proliferating cells; required for resistance to bleomycin, may be involved in protecting against oxidative damage; similar to mammalian PA200	0.071773
ERV46	-1.33914	Protein localized to COPII-coated vesicles; forms a complex with Erv41p; involved in the membrane fusion stage of transport	0.07787
AUA1	-2.3285	Protein required for the negative regulation by ammonia of Gap1p; Gap1p is a general amino acid permease	0.07787
DUS1	-1.8118	Dihydrouridine synthase; member of a widespread family of conserved proteins including Smm1p, Dus3p, and Dus4p; modifies pre-tRNA(Phe) at U17	0.078521
RIT1	-0.91525	Initiator methionine 2'-O-ribosyl phosphate transferase; modifies the initiator methionine tRNA at position 64 to distinguish it from elongator methionine tRNA	0.080721
GFD1	-7.71107	Coiled-coiled protein of unknown function; identified as a high-copy suppressor of a dbp5 mutation; protein abundance increases in response to DNA replication stress	0.084632
*BUD20**	-1.08013	C2H2-type zinc finger protein required for ribosome assembly; shuttling factor which associates with pre-60S particles in the nucleus, accompanying them to the cytoplasm	0.084826
LAG2	-1.51709	Protein that negatively regulates the SCF E3-ubiquitin ligase; regulates by interacting with and preventing neddyation of the cullin subunit, Cdc53p	0.08986
CLG1	-5.32648	Cyclin-like protein that interacts with Pho85p; has sequence similarity to G1 cyclins PCL1 and PCL2	0.08986
MET6	-5.89835	Cobalamin-independent methionine synthase; involved in methionine biosynthesis and regeneration; requires a minimum of two glutamates on the methyltetrahydrofolate substrate, similar to bacterial metE homologs	0.091724
RVS167	-3.59454	Calmodulin-binding actin-associated protein; roles in endocytic membrane tabulation and constriction, and exocytosis	0.092565
BSC1	-2.2407	Protein of unconfirmed function; similar to cell surface flocculin Flo11p;	0.093217

ELP6	-1.01899	Subunit of hexameric RecA-like ATPase Elp456 Elongator subcomplex; which is required for modification of wobble nucleosides in tRNA;	0.09526
SHH3	-1.57505	Putative mitochondrial inner membrane protein of unknown function	0.095407

[1.]Genes in bold encode proteins whose cellular locations are affected by DNA replication stress , *Appears Twice Among Screens ($q < 0.1$), **Appears Twice Among Screens ($q < 0.1$ and $p < 0.05$)

[2.]m.value is the numeric vector of fold change on a log2 scale

[3.]q value is the numeric vector calculated based on the p-value using the p.adjust function with default parameter settings.

Table 3. Top 15 Gene Ontology Groups According to the Yeast GO-Slim Process

GO-Slim term[1.]	Genes annotated to the term
Cellular response to DNA damage stimulus	*CKB1, CKB2, CSM2, DPB3, NUP60, PSY2, PSY3, RAD1, RAD10, RAD17, RAD18, RAD2, RAD4, RAD5, RAD54, RAD55, REV1, REV3*
DNA repair	*CSM2, DPB3, NUP60, PSY2, PSY3, RAD1, RAD10, RAD17, RAD18, RAD2, RAD4, RAD5, RAD54, RAD55, REV1, REV3*
Meiotic cell cycle	*CLB5, CSM2, DIT1, HHF1, PSY2, RAD1, RAD10, RAD17, RAD55, SPO1, SWM1, V PS13*
Response to chemical	*CUE1, DAL82, GRE3, PSY2, RAD23, SSM4, SVF1, TRM9, TRX3*
Transcription from RNA polymerase II promoter	*DAL82, DST1, ELP6, FKH2, HHF1, RAD2, RAD23, RAD4*
Organelle fission	*CLB5, CSM2, PSY2, RAD1, RAD10, RAD17, RAD55, SWM1*
DNA recombination	*CSM2, PSY3, RAD1, RAD10, RAD17, RAD54, RAD55*
Protein complex biogenesis	*ATP11, BLM10, DST1, RAD5, RAV1, TCM62, VOA1*
Proteolysis involved in cellular protein catabolic process	*BLM10, CUE1, RAD23, RAD4, RPN10, SSM4, SWM1*
Biological process unknown	*BSC1, MIX23, NRP1, PIB2, SHH3, SKG3, YOR041C*
Regulation of cell cycle	*BCK2, CLB5, FKH2, PSY2, RAD17, SWM1*
Mitotic cell cycle	*BCK2, BUD20, CLB5, FKH2, MNN10, SWM1*
Protein modification by small protein conjugation or removal	*ELP6, LAG2, NUP60, RAD18, RAD5, SWM1*

Carbohydrate metabolic process	*GRE3, GTB1, HXK2, PPG1, ROT2*
Chromatin organization	*DPB3, FKH2, HHF1, NUP60, RAD54*

[1.] See http://www.yeastgenome.org/goSlimMapper

Table 4. Protein Complexes That Participate in AFB_1 Resistance

GO-term	Description[1.]	Count in gene set	False discovery rate
GO:1990391	DNA repair complex	7 of 28	5.22E-05
GO:0000109	Nucleotide-excision repair complex	5 of 16	0.00063
GO:0017177	Glucosidase II complex	2 of 2	0.0214
GO:0000111	Nucleotide-excision repair factor 2 complex	2 of 3	0.0299
GO:0000110	Nucleotide-excision repair factor 1 complex	2 of 3	0.0299
GO:0005956	Protein kinase CK2 complex	2 of 4	0.0385
GO:0097196	Shu complex	2 of 4	0.0385

[1.] See http://www.yeastgenome.org/goSlimMapper and https://string-db.org/

Table 5. Enrichment of DNA Damage Repair Genes Among AFB_1 Resistant Genes

GO Biological Process[1.]	Yeast	AFB_1 Resistant Genes	Expected	Fold Enrichment	P value	Significance
Error-prone translesion synthesis	11	5	<1	>5	3.62E-04	+
Translesion synthesis	18	5	<1	>5	4.00E-03	+
DNA synthesis involved in DNA repair	20	5	<1	>5	6.67E-03	+
DNA repair	285	15	3.10	4.85	8.12E-04	+
DNA metabolic process	495	17	5.38	3.16	3.99E-02	+
Cellular process	4675	66	50.78	1.30	4.53E-02	+
Cellular response to DNA damage stimulus	331	18	3.60	5.01	2.63E-05	+
Cellular response to stress	673	23	7.31	3.15	8.74E-04	+
Response to stress	764	23	8.30	2.77	7.92E-03	+
Postreplication repair	29	5	<1	>5	3.96E-02	+
Error-prone translesion synthesis	11	5	<1	>5	3.62E-04	+
Translesion synthesis	18	5	<1	>5	4.00E-03	+
DNA synthesis involved in DNA repair	20	5	<1	>5	6.67E-03	+
Unclassified	733	1	7.96	< 0.2	0.00E00	-

[1.] See http://pantherdb.org/tools/ for statistical analysis

Table 6. Human Genes Orthologous to Yeast Resistance Genes

Yeast Gene[1.]	Human Gene[2.]	Description/Function
AKL1	AAK1	Adaptor protein 2 associated kinase 1
ATP11	ATPAF1	F1-ATPase assembly factor 1
ATP15	ATP5E	ϵ subunit of human ATP synthase
BLM10	PSME4	Proteasome activator complex subunit 4
CIN4	ARL2-SNX15	ADP Ribosylation Factor-like Protein
HHF1	HIST1H4D	Histone H4
CKB1	CSNK2B	Casein kinase II subunit beta
CKB2	CSNK2B	Casein kinase II subunit beta
CLB5	CCNB1, CCNB2	G2/mitotic-specific cyclin-B2
DST1	TCEA1	Transcription elongation factor A1
*DPB3**	CHRAC1	Chromatin accessibility complex protein 1
FKH2	FOXE1	Forkhead box protein E1
FUM1	FH	Fumarate hydratase, mitochondrial
GLO1	GLO1	GLyOxalase
GRE3	AKRA1,B1,D1, E2, B10	Aldo-keto reductase family 1 member, A1, B1, D1, E2, B10
GTB1	PRKCSH	Protein kinase C substrate 80K-H
MIS1	MTHFD1	Methylenetetrahydrofolate dehydrogenase
MIX23	CCDC58	Coiled-coil domain-containing protein 58
MRPL35	MRPL38	Large subunit mitochondrial ribosomal protein L38
MYO4	MYO5A	Unconventional myosin-Va
NRP1	TEX13B	N (asparagine)-Rich Protein, Testis-expressed protein 13B
PEX3	PEX3	Peroxisomal biogenesis factor 3
PPG1	PPP2CB	Protein Phosphatase involved in Glycogen accumulation
PSY2	PPP4R3B	Serine/threonine-protein phosphatase 4 regulatory subunit 3B
RAD1	ERCC4	DNA repair endonuclease XPF
RAD2	ERCC5	DNA repair protein complementing XP-G cells
RAD4	XPC	DNA repair protein complementing XP-C cells
RAD5	HLTF	Helicase-like transcription factor involved in DNA damage tolerance
RAD10	ERCC1	Excision Repair Cross-Complementing 1 ERCC1
RAD17	RAD1	Cell cycle checkpoint protein RAD1
RAD18	RAD18	E3 ubiquitin-protein ligase RAD18
RAD23	RAD23A	UV excision repair protein RAD23 homolog A
RAD54	RAD54L	DNA repair and recombination protein RAD54-like

RAD55	RAD51B	DNA repair protein RAD51 paralog B
RAV1	DMXL2	Dmx like 2 also known as rabconnectin-3, involved in vacuolar acidification
REV1	REV1	REV1, DNA directed polymerase
REV3	REV3L	REV3 Like, DNA directed polymerase zeta catalytic subunit
RNR3	RRM1	Ribonucleotide reductase catalytic subunit M1
ROT2	GANAB	Glucosidase alpha, neutral C
RPN10	PSMD4	26S proteasome non-ATPase regulatory subunit 4
RPS4A	RPS4X	Ribosomal Protein of the Small subunit , 40S ribosomal protein S4, X isoform
SKG3	STK39	Serine/threonine kinase 39
SPO1	PLA2G4A	Phospholipase A2 group IVA
SSM4	MARCH6	Membrane associated ring-CH-type finger 6
TES1	ACOT8	Acyl-coenzyme A thioesterase 8
TMA20	MCTS1	Malignant T-cell-amplified sequence 1, translation re-initiation and release factor
TRM9	ALKB8	Alkylated DNA repair protein alkB homolog 8
VPS13	VPS13A	Vacuolar protein sorting 13 homolog A
YIH1	IMPACT	Impact RWD domain protein**;** translational regulator that ensures constant high levels of translation upon a variety of stress conditions; impact RWD domain protein
YND1	ENTPD4 and ENTPD7	Ectonucleoside triphosphate diphosphohydrolase 4 and 7

[1.] For full description, see Table 2.

[2.] Human genes derived from https://www.alliancegenome.org/gene/SGD:S000004022

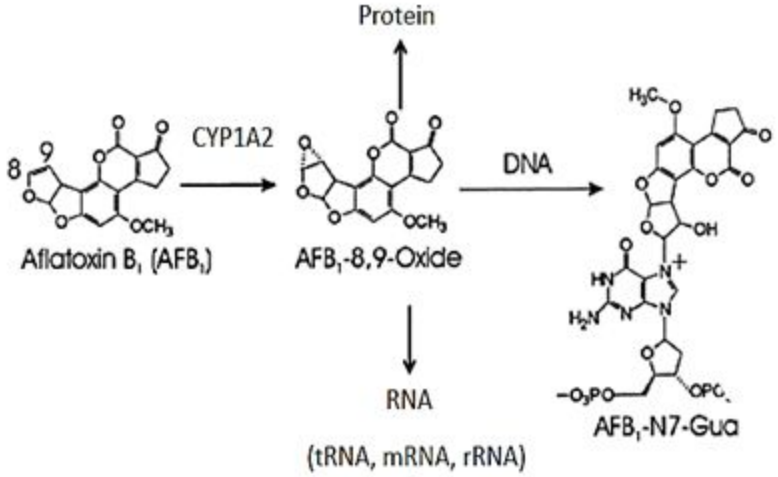
Protein
CYP1A2
DNA
Aflatoxin B1 (AFB1)
AFB1-8,9-Oxide
AFB1-N7-Gua
RNA
(tRNA, mRNA, rRNA)

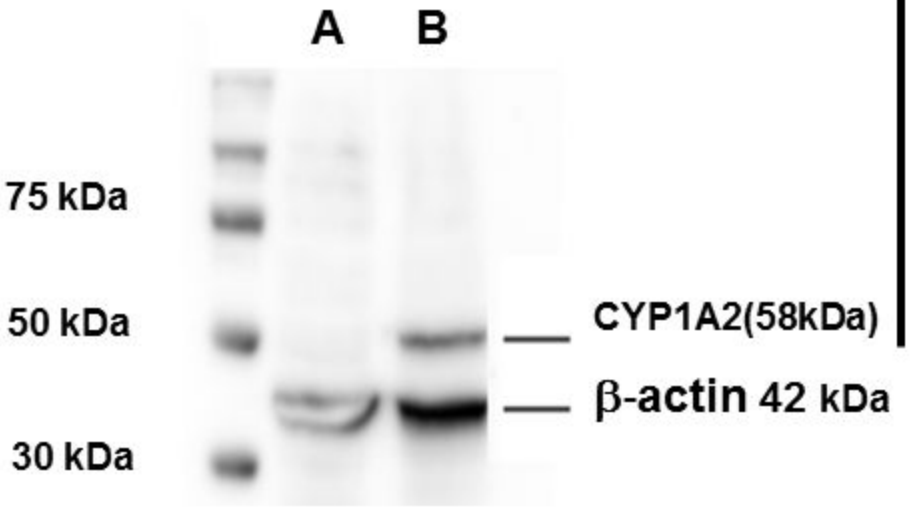
A
B
75 kDa
50 kDa
30 kDa
CYP1A2(58kDa)
β-actin 42 kDa

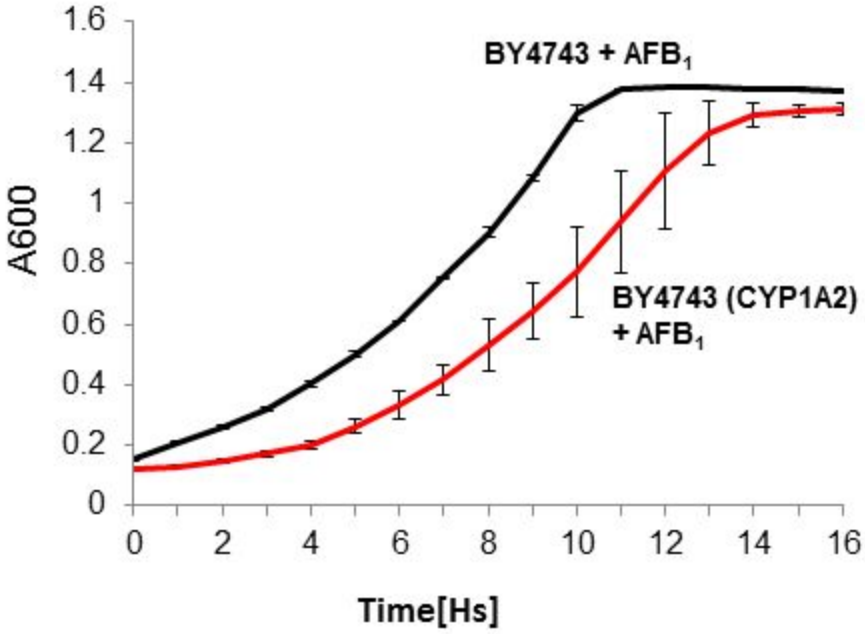
BY4743 + AFB1
BY4743 (CYP1A2) + AFB1
A600
Time[Hs]

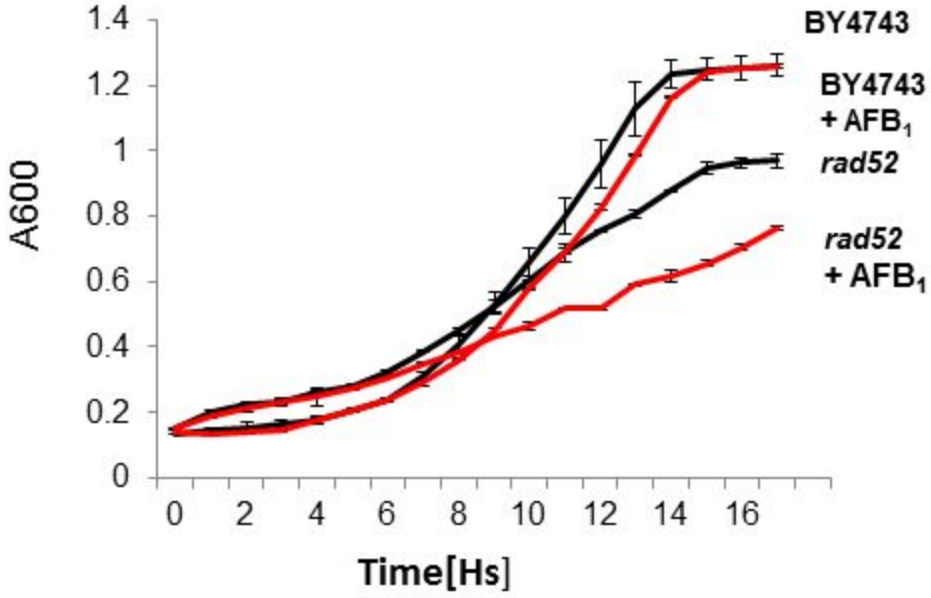
BY4743
BY4743 + AFB1
rad52
rad52 + AFB1
A600
Time[Hs]

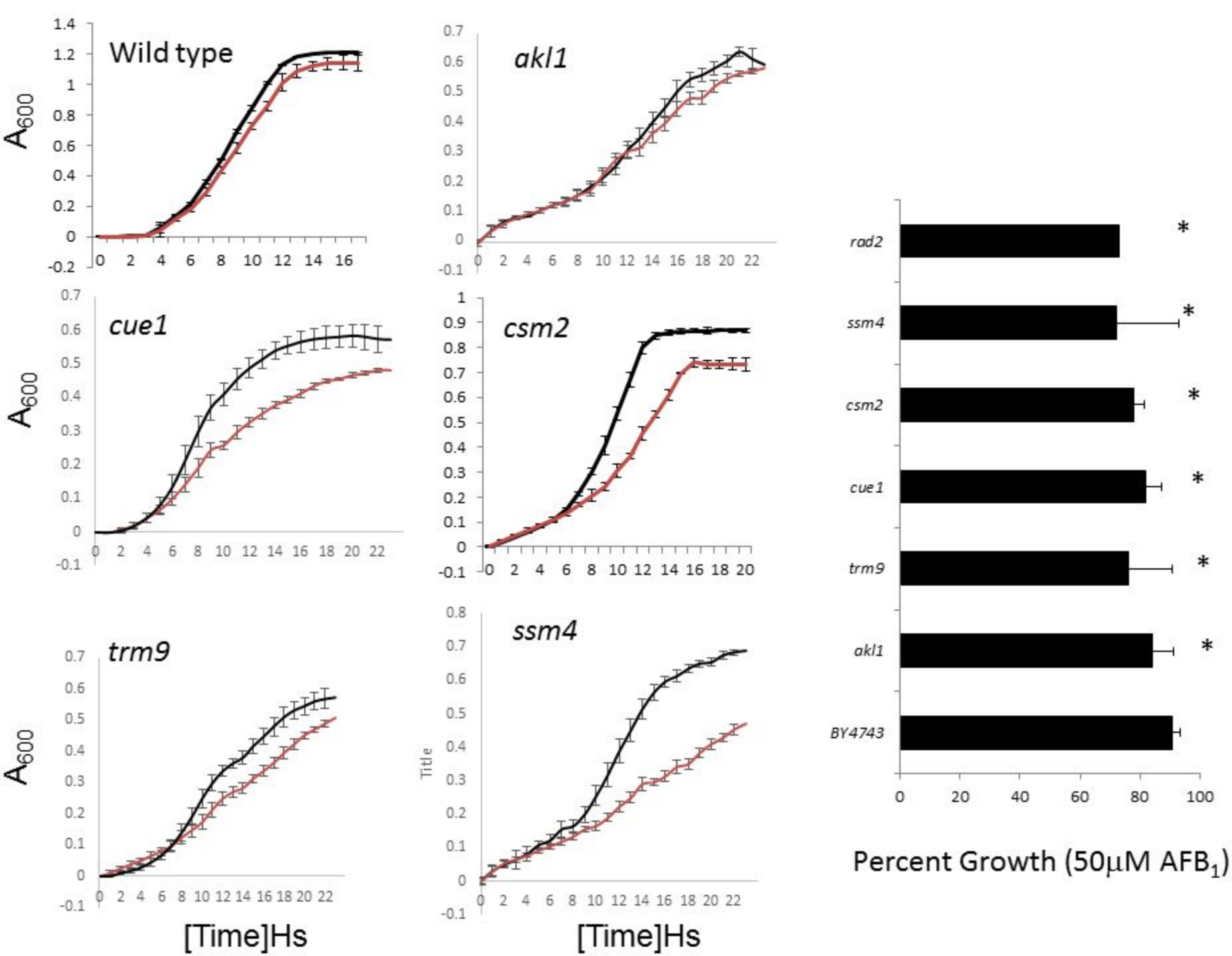
Wild type
akl1
cue1
csm2
trm9
ssm4
A600
[Time]Hs
rad2
ssm4
csm2
cue1
trm9
akl1
BY4743
Percent Growth (50μM AFB1)

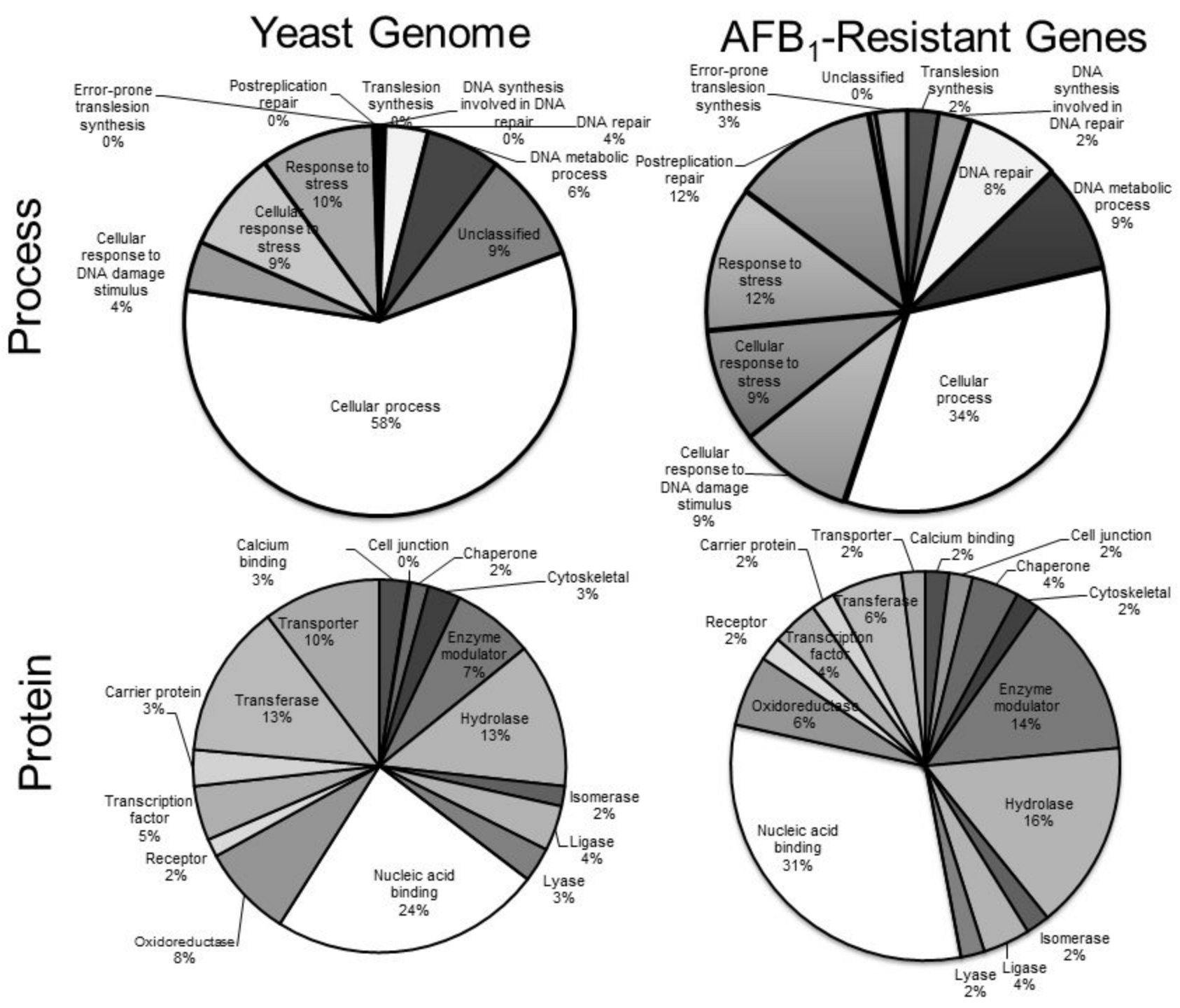
Yeast Genome
AFB1-Resistant Genes
Process
Protein
Error-prone translesion synthesis 0%
Postreplication repair 0%
Translesion synthesis 0%
DNA synthesis involved in DNA repair 0%
DNA repair 4%
DNA metabolic process 6%
Unclassified 9%
Cellular process 58%
Cellular response to DNA damage stimulus 4%
Cellular response to stress 9%
Response to stress 10%
Error-prone translesion synthesis 3%
Unclassified 0%
Translesion synthesis 2%
DNA synthesis involved in DNA repair 2%
DNA repair 8%
DNA metabolic process 9%
Postreplication repair 12%
Response to stress 12%
Cellular response to stress 9%
Cellular process 34%
Cellular response to DNA damage stimulus 9%
Calcium binding 3%
Cell junction 0%
Chaperone 2%
Cytoskeletal 3%
Transporter 10%
Enzyme modulator 7%
Carrier protein 3%
Transferase 13%
Hydrolase 13%
Isomerase 2%
Transcription factor 5%
Ligase 4%
Receptor 2%
Lyase 3%
Nucleic acid binding 24%
Oxidoreductase 8%
Carrier protein 2%
Transporter 2%
Calcium binding 2%
Cell junction 2%
Chaperone 4%
Cytoskeletal 2%
Transferase 6%
Receptor 2%
Transcription factor 4%
Enzyme modulator 14%
Oxidoreductase 6%
Hydrolase 16%
Nucleic acid binding 31%
Isomerase 2%
Lyase 2%
Ligase 4%

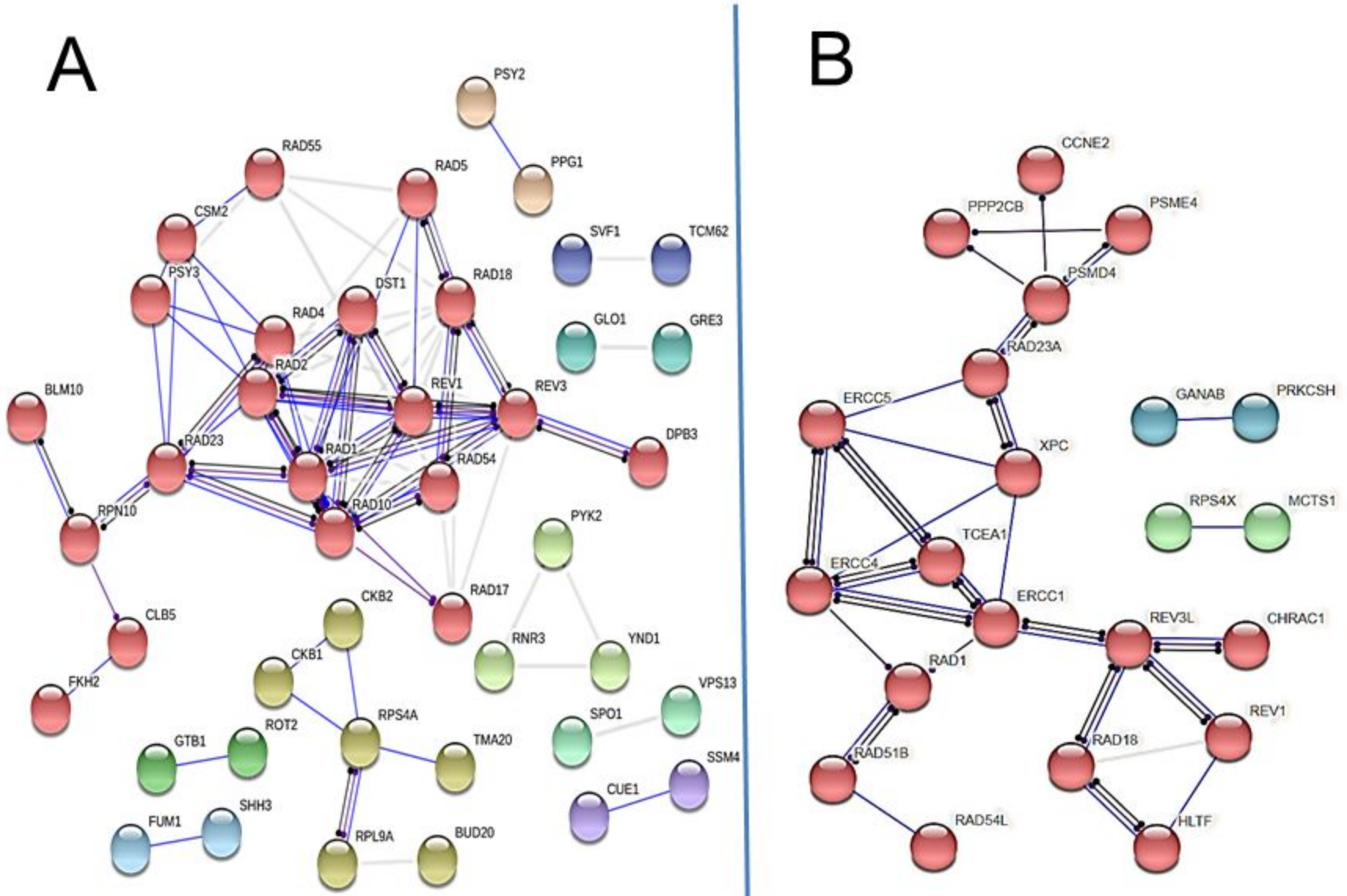
A
PSY2
PPG1
RAD55
RAD5
CSM2
SVF1
TCM62
PSY3
DST1
RAD18
RAD4
GLO1
GRE3
RAD2
REV1
REV3
BLM10
DPB3
RAD23
RAD1
RAD54
RAD10
RPN10
PYK2
CKB2
RAD17
CLB5
RNR3
YND1
CKB1
FKH2
VPS13
RPS4A
SPO1
GTB1
ROT2
TMA20
SSM4
CUE1
SHH3
FUM1
RPL9A
BUD20
B
CCNE2
PPP2CB
PSME4
PSMD4
RAD23A
ERCC5
GANAB
PRKCSH
XPC
RPS4X
MCTS1
TCEA1
ERCC4
ERCC1
REV3L
CHRAC1
RAD1
REV1
RAD18
RAD51B
RAD54L
HLTF

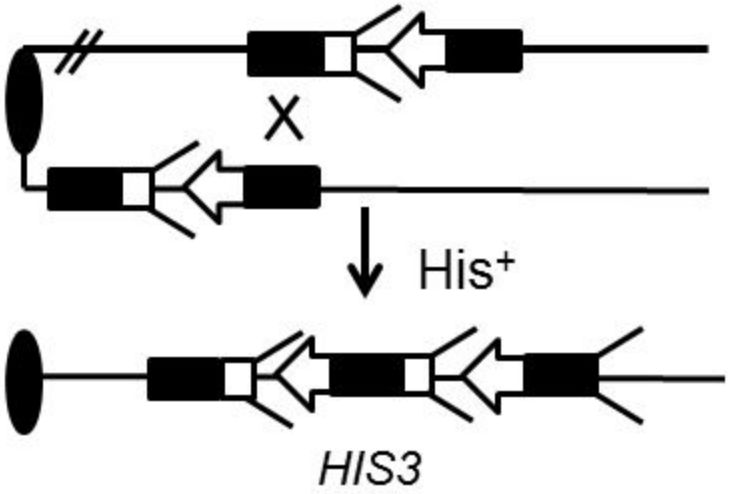
X
His+
HIS3

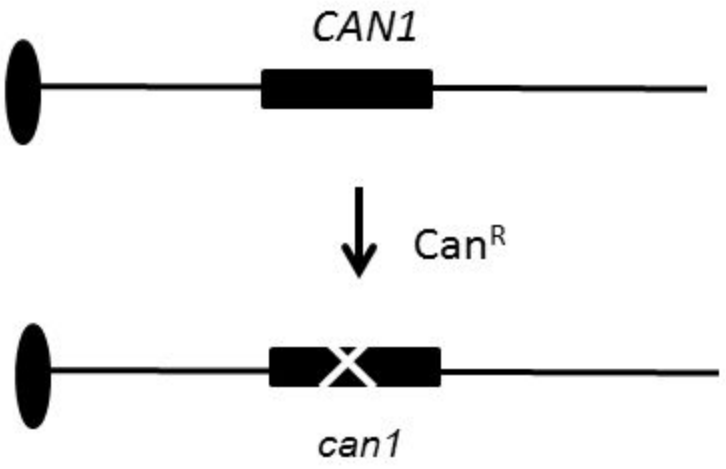
CAN1
CanR
can1

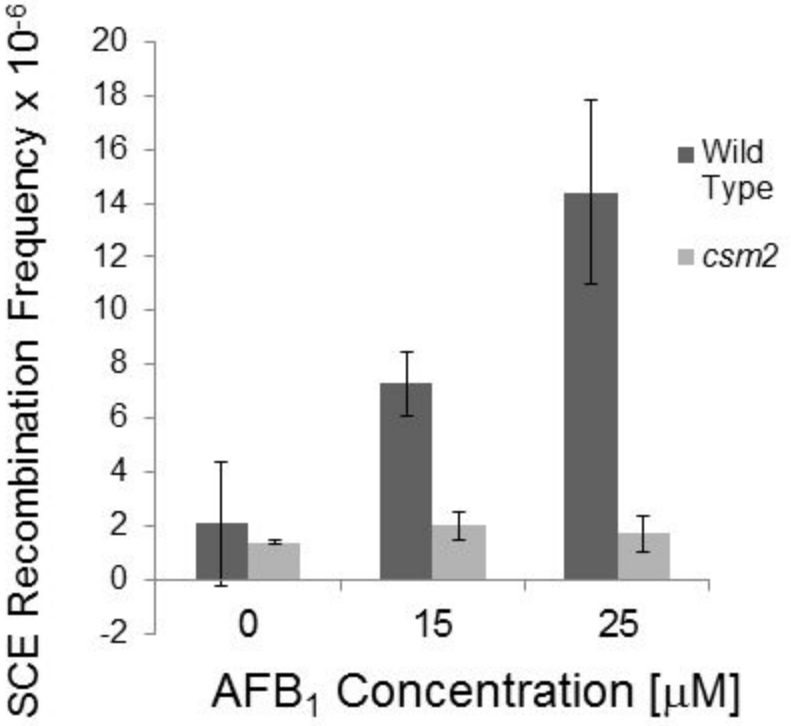
SCE Recombination Frequency x 10-6
20
18
16
14
12
10
8
6
4
2
0
-2
0
15
25
AFB1 Concentration [μM]
Wild Type
csm2

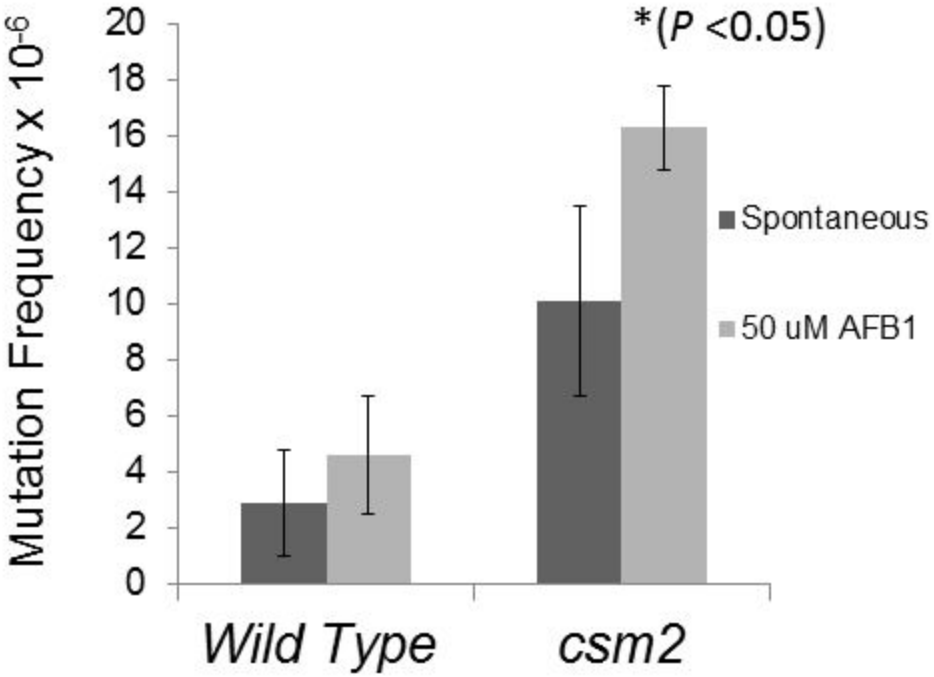
Mutation Frequency x 10-6
*(P <0.05)
20
18
16
14
12
10
8
6
4
2
0
Wild Type
csm2
Spontaneous
50 uM AFB1

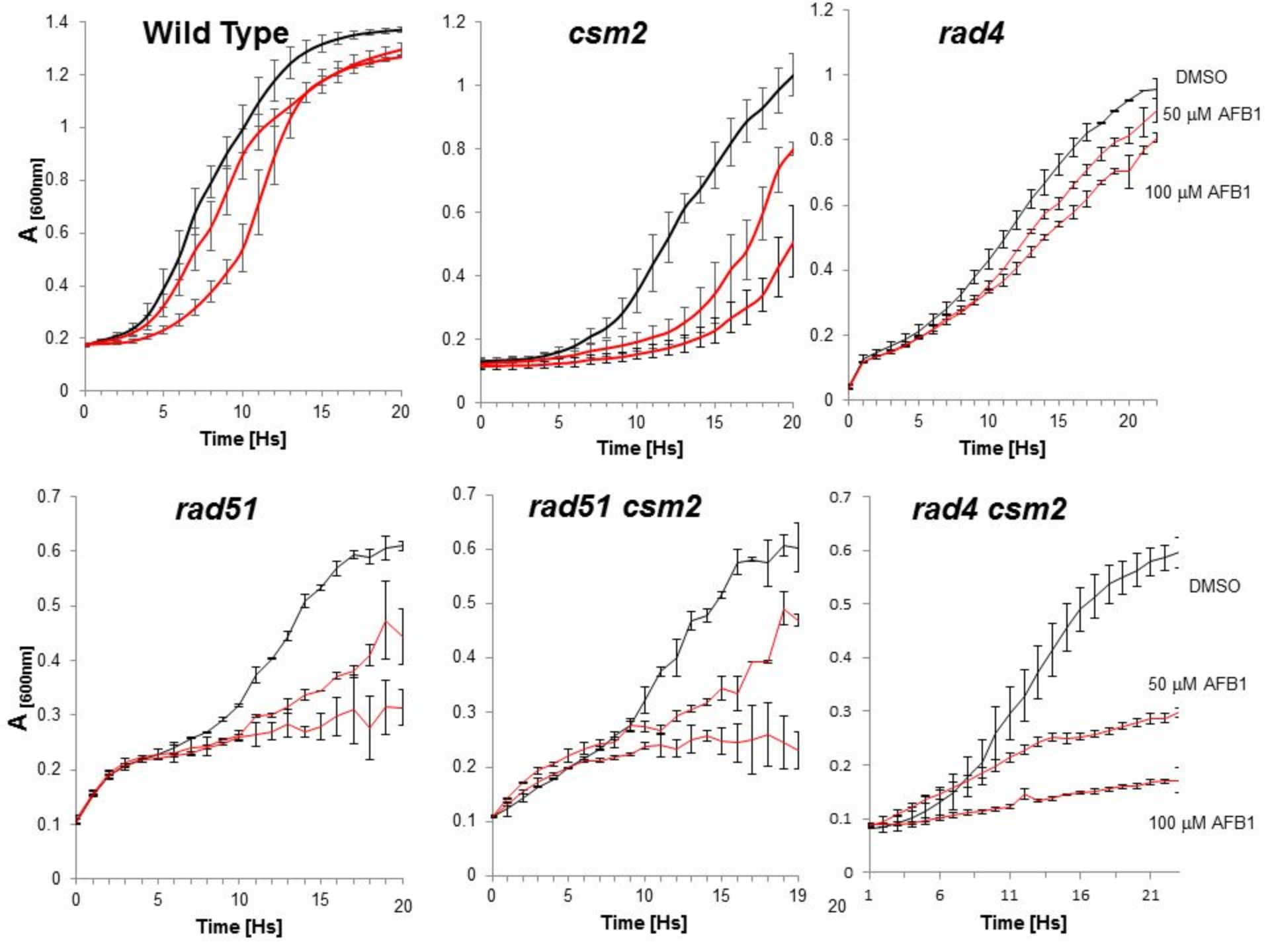
Wild Type
csm2
rad4
rad51
rad51 csm2
rad4 csm2
A [600nm]
Time [Hs]
DMSO
50 µM AFB1
100 µM AFB1